Zeitschrift: IABSE reports = Rapports AIPC = IVBH Berichte
Band: 59 (1990)

Rubrik: Theme B: Behaviour of materials

THEME B

Behaviour of Materials

Comportement des matériaux

Materialverhalten

Leere Seite
Blank page
Page vide

Experimental and Theoretical Investigations of Existing Railway Bridges

Recherche théoriques et expérimentales sur des ponts de chemin de fer existants

Experimentelle und theoretische Untersuchungen an bestehenden Eisenbahnbrücken

Friedrich MANG
Prof. Dr.-Eng.
Univ. of Karlsruhe
Karlsruhe, Fed. Rep. of Germany

Friedrich Mang, born 1934, received his civil engineering degree at the University of Karlsruhe.

Oemer BUCAK
Dipl.-Eng.
Univ. of Karlsruhe
Karlsruhe, Fed. Rep. of Germany

Oemer Bucak, born 1947, received his civil engineering degree at the University of Karlsruhe.

SUMMARY
This paper describes an investigation of a complete bridge structure of the «museum railway» in the community of Blumberg as well as two bridge structures of the «Deutsche Bundesbahn». Results of component tests are compared with data taken from the literature as well as other results of similar investigations.

RÉSUMÉ
Cet article présente une recherche effectuée sur une structure complète d'un pont du «musée du chemin de fer» de la commune de Blumberg, ainsi que sur deux structures de ponts de la «Deutsche Bundesbahn». Les résultats des essais effectués sur ces éléments sont comparés avec les valeurs provenant de la littérature, ainsi qu'avec celles tirées d'autres essais de recherches similaires.

ZUSAMMENFASSUNG
Der Bericht handelt von Untersuchungen an einem kompletten Brückenbauwerk der «Museumsbahn» der Gemeinde Blumberg sowie an zwei Brückenelementen der «Deutschen Bundesbahn». Die Resultate werden mit bekannten Angaben aus der Literatur sowie mit weiteren Ergebnissen ähnlicher Untersuchungen verglichen.

1. PRELIMINARY REMARKS

All over the world the industrialization starting early in the 20th century paved the way for numerous constructions, particularly for steel railway bridges. Still today we find bridges dating from the end of the last century, i.e. about 1850. These bridges are mainly riveted constructions designed for low external loads. The standard service lives of these constructions were short compared to current designs. In many cases, however, they have been exceeded by far. All over Europe we find bridges which have been continuously in service for more than 100 years. Most of these buildings are classified as historical monuments or shall be preserved for economical reasons.

In most cases it is impossible to make a definitive judgement as to whether a construction under fatigue loading can be used further after its standard service life has been reached or exceeded. Further problems occur when the safety of an old bridge has to be recalculated due to increased design loads (e.g. new load spectra for trains) or when the safety of a building damaged in an accident has to be estimated. This can be explained by the poor knowledge of the static strength and the fatigue strength of steels (wrought iron, puddled iron) and constructional details (X lattice girders, rivet joints) used in the 19th century.

The judgement of old bridges is based on results of material tests on specimens taken from areas under low loading conditions, such as bracings and support areas. Up to the present, these data have been reduced by high safety factors to obtain a safe estimation. The structural design of the connections has a considerable influence on the load-carrying capacity of the whole construction. Till today tests on whole constructions and their connections have been carried out only sporadically.

"Damage" or "fatigue" incurred during the service life are determined by means of hypotheses the reliability of which is not quite indisputed. Data on the load history of bridges built during the two world wars and in early post-war times are not available. The judgement is therefore based on mean values and estimated load histories. In order to be on the safe side, we try today to obtain the required data by tests on all structural components under high loading conditions.

2. DETERMINATION OF THE REMAINING SERVICE LIFE OF A FATIGUE-LOADED CONSTRUCTION

Up to a short time ago, the procedure to determine the remaining service life of a bridge was as follows:

- visual inspection of the bridge, outward appearance (corrosion), with some bridges this was the dominating point of judgement
- specification of repairs or reinforcement measures (e.g. due to increased loads from engine and cars)
- determination of points under maximum stress (by means of the design calculation or by new calculation e.g. according to BE 804); determination of points governing the safety of the construction (e.g. tensile members); for highway bridges see DIN 1072 and DIN 18809 taking account of impact loads and crash barrier spacings
- taking of specimens from uncritical, but representative areas of the construction
- tests, e.g. chemical analysis, tension test and fatigue tests, on the original material
- additional calculations based on actual material properties
- determination of the previous load history and future loads

- determination of the remaining service life using Miner's linear cumulative damage rule and fixing of a safety factor for the respective bridge construction
- fixing of inspection intervals
- fracture-mechanical tests, e.g. COD tests, determination of the critical crack size, previous damages.

Defective structural components (damaged e.g. by corrosion, by accident (see Fig. 1) or by bullets) may cause a considerable reduction of the life of a construction depending on the situation of the defect and on the stress level. We therefore recommend to attach special importance to these points when visiting a construction.

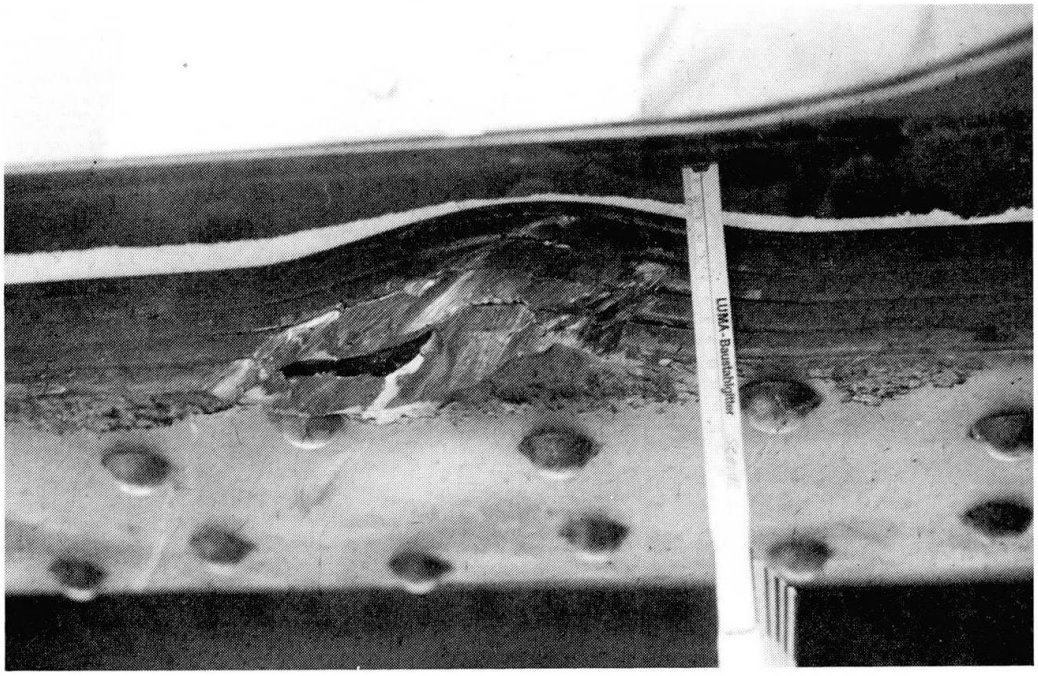

Fig. 1 Bridge damaged by impact

Certificates on various constructions under high-cycle fatigue loading and tests carried out for a research program |1| supplied sufficient data on the material properties thus allowing a preliminary estimation. Therefore, only few tests in the final stage are necessary to confirm these presumptions. The load-carrying behaviour of such constructions as a whole and the load-carrying capacity of structural components in the original state are not yet sufficiently known. The points in question are: rivet slip, rivet preloading, displacement under shear load, distribution of the load to other elements of a structural component. Large structural components should therefore be investigated as a whole.

At the "Versuchsanstalt für Stahl, Holz und Steine" tests were carried out on a whole bridge built in 1887 which had been chosen from different bridge systems of the "Museumsbahn" (Fig. 2).

Fig. 2 Bridge of the "Museumsbahn"

3. FATIGUE TESTS AND RESULTS

3.1 Tests on the whole bridge

The whole bridge was built in the 50 MN power press of the institute. Fig. 3 shows the bridge built in according to load configuration LF 1.

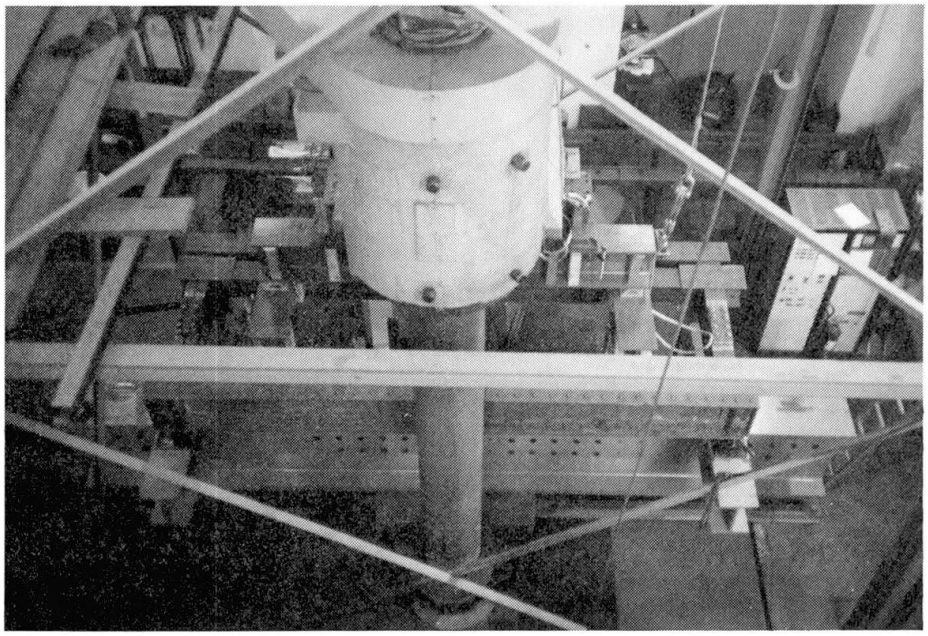

Fig. 3 Bridge of the "Museumsbahn" in the 50 MN power press

The test was interrupted at 108 070 stress cycles as a correct load application was no longer possible due to a large crack in the connection between transverse girder and main girder. Fig. 4 shows the point of failure.

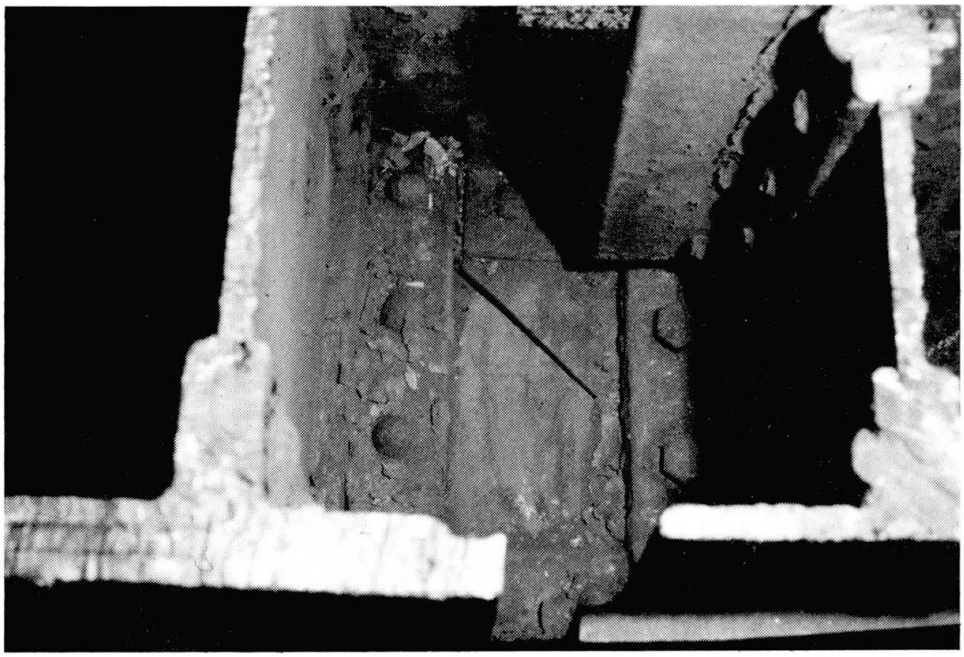

Fig. 4 Connection between transverse girder and main girder, crack in web plate

Afterwards, the bridge was sawed up (see Fig. 5) to carry out seperate tests on components (main girder, longitudinal girder) and connections (transverse girder, main girder).

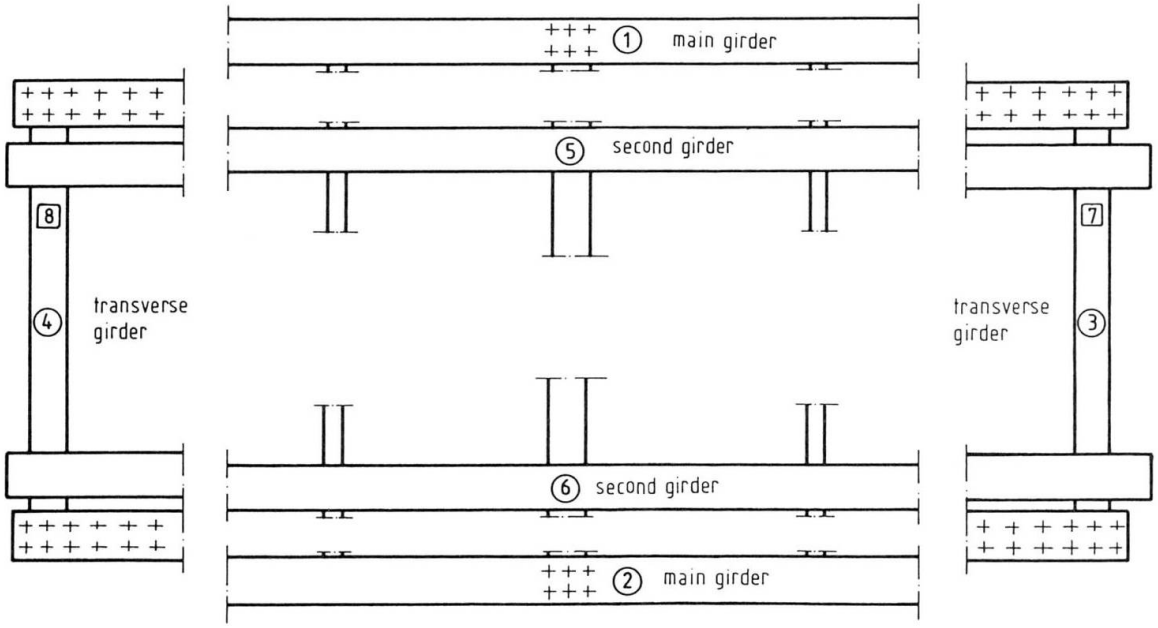

Fig. 5 Blumberg bridge - designation of specimens

Analogously, the Stahringen bridge dating from 1895 was sawed up to investigate the two main girders and the connections between main girder and transverse girder. Fig. 6 shows the components of one half of the bridge. Punched specimens, riveted specimens as well as specimens of the plain web plate material were taken from the remaining bridge parts.

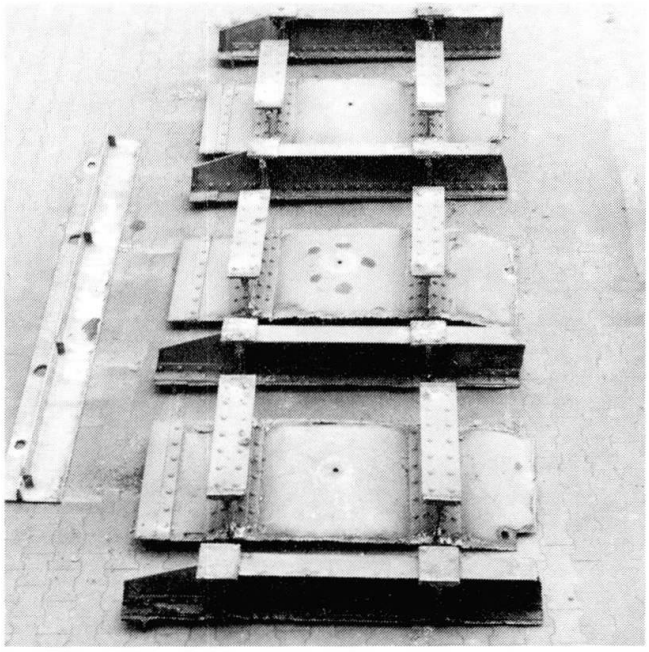

Fig. 6 Stahringen bridge - structural components

3.2 Tests on the main girder

The main girders of the two bridges were subjected to four-point-bending tests with a span of 3300 mm. The spacing between the two points of load application was 800 mm. The tests were carried out on two stress levels (135 N/mm² and 165 N/mm²) with an ultimate stress ratio of R = + 0.2.

In these cases the fatigue crack usually started from a rivet hole in the tension chord due to a stress concentration in the hole rim. The punching and riveting procedures as well as corrosion may also cause damages in the hole rim. An exception to this rule are those cases where components have been seriously damaged e.g. by impact or by bomb splinters.

Under a maximum stress of 165 N/mm² and at 1 534 000 stress cycles the crack occurred in the web of main girder I of the Blumberg bridge. Despite the crack, the main girder carried the full load and the test was continued until the two angles and the cover plate of the main girder tensile chord failed at a total number of stress cycles of 1 572 600. This means that the minimum number of stress cycles between crack appearance and total failure of the main girder was 38 600 (see Fig. 7).

Fracture first occurred in the web, then in the angle section and finally in the cover plate. The cracks were not situated on one level.

Subsequently, the main girder II of the Museumsbahn bridge and the two main girders of the Stahringen bridge were tested under the same conditions. The first crack occurred in the main girder web. The numbers of stress cycles between crack appearance and total failure of the main girder ranged up to 100 000.

Three additional specimens were taken from the uncracked main girder parts of the Blumberg bridge. These specimens were subjected to three-point-bending tests with a span of 1500 mm. The maximum loads were 450 kN and 600 kN, the ultimate stress ratios were R = + 0.35 and R = + 0.1. These test results will help in judging the influence of the mean stress.

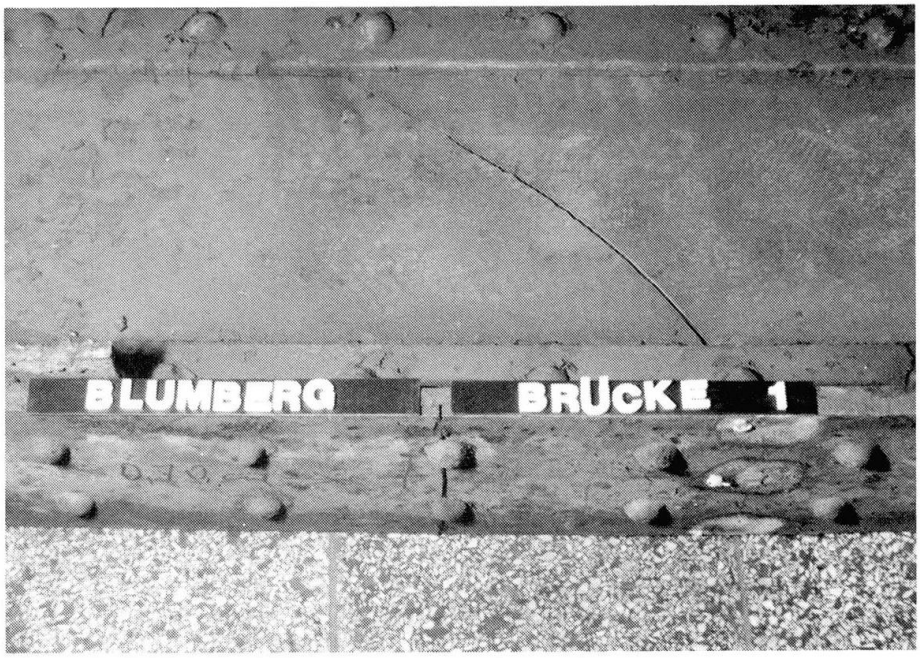

Fig. 7 Points of fracture of main girder I

Fig. 8 shows the test results in comparison with earlier data obtained by tests on punched specimens of puddled iron. The diagram shows that the results of the main girder and transverse girder tests are within the range of scattering of results for small-scale specimens.

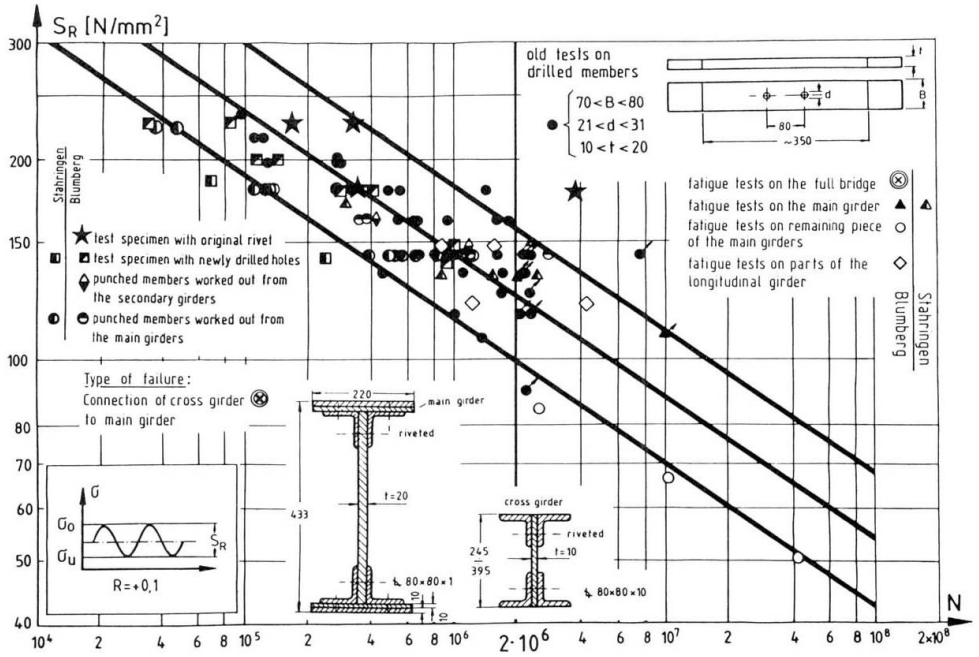

Fig. 8 Results of tests on components of the Blumberg bridge compared to earlier test results of punched specimens

The results of the specimens taken from the remaining parts of the main girder are slightly beyond the $P_{ü}$ = 97.5 % line which is due to previous fatigue loads endured during service and during the girder tests (1.6 to $2.0\cdot10^6$ stress cycles).

3.3 Tests on transverse girder connections

In the tests on the whole bridge failure occurred at the transverse girder connections. These connections were therefore a point of major consideration in the investigation of the service life of bridges. Full details of these investigations are given in |10|.

3.4 Tests on parts of the longitudinal girders

Four specimens were taken from the longitudinal girders of the Museumsbahn bridge and subjected to three-point-bending tests with a span of 1500 mm. For two specimens the maximum stress was 165 N/mm², for the other ones 135 N/mm². The ultimate stress ratio was R = + 0.1. The test results are shown in Fig. 8 in comparison with earlier data for flat plate specimens of similar age. The cracks usually started at a distance of about 600 mm from the point of support and proceeded diagonally through the web. In some specimens further cracks occurred in the angle sections. Fig. 9 gives an example of the failure mode.

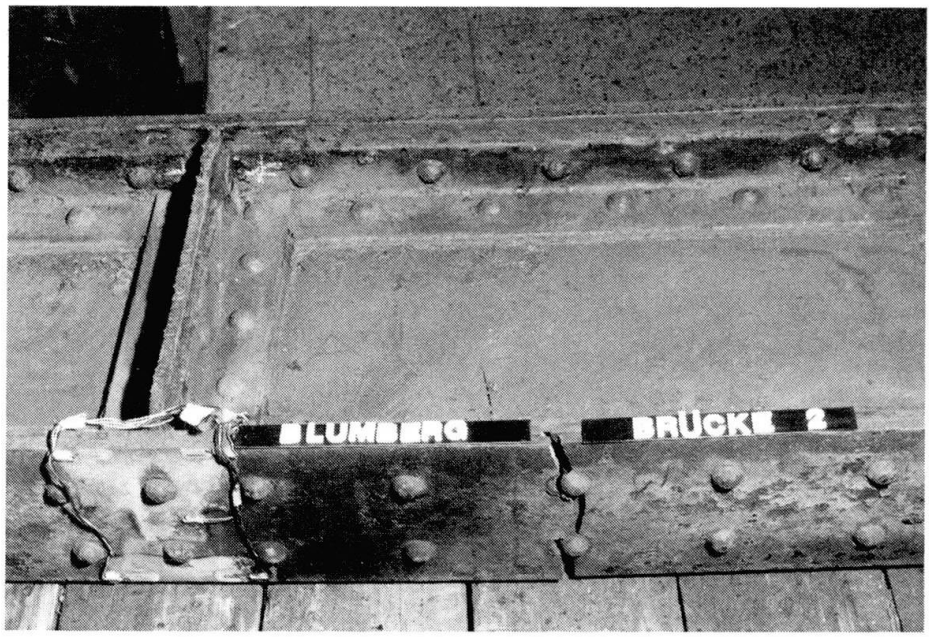

Fig. 9 Failure mode for the longitudinal girder of the Blumberg bridge

3.5 Tests on riveted and punched specimens

The central parts of wind bracings of the bridge were fatigue tested in the original state (with rivets) in a pulsator.

The remaining material of the bracings was used for punched specimens, i.e. specimens with new holes ∅ 20 mm, which were fatigue tested at different stress levels.

Further specimens with original holes were taken from remaining parts of main girders and longitudinal girders. The results of these tests are plotted in Fig. 10.

It is evident that the test results are in good agreement with earlier data, although the data of the Stahringen bridge are comparatively low. The scattering of the results is comparatively large, as is the rule with old constructions.

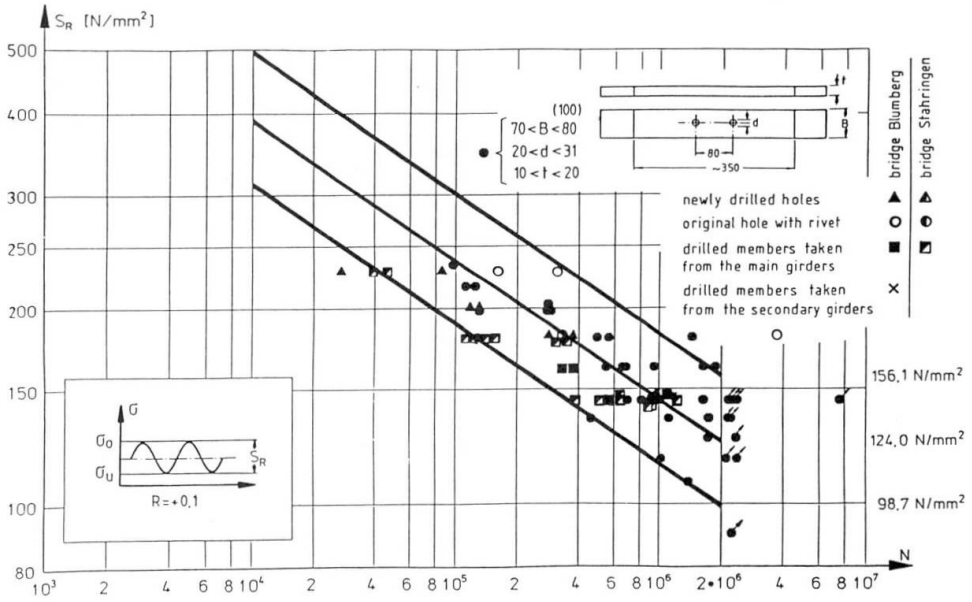

Fig. 10 Results of tests on punched specimens and specimens with original rivets

Two specimens taken from the web area are also in good agreement with earlier test data. As expected, the fatigue cracks started from rivet holes. Fig. 11 shows the specimens taken from the main girder of the Stahringen bridge after failure. After the first crack had occurred the specimens were re-fixed until a second or a third crack started from another rivet hole.

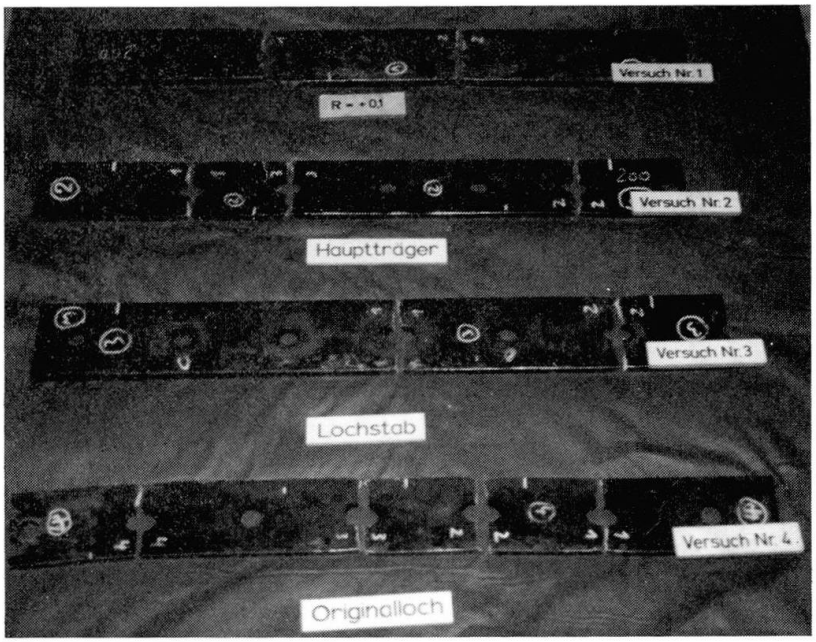

Fig. 11 Specimen after failure (punched specimen from Stahringen bridge)

4. COMPARATIVE TEST DATA FROM THE LITERATURE

As mentioned before, information on the fatigue behaviour of old steels, particularly from the 19th century is very scarce. Hirt and Brühwiler |3| were the first researchers to carry out a methodical evaluation for two old bridge components. They compared their results to those of three other reports. For comparison the test results of the Blumberg bridge and the Stahringen bridge were entered into the diagrams of Figs. 12 and 13.

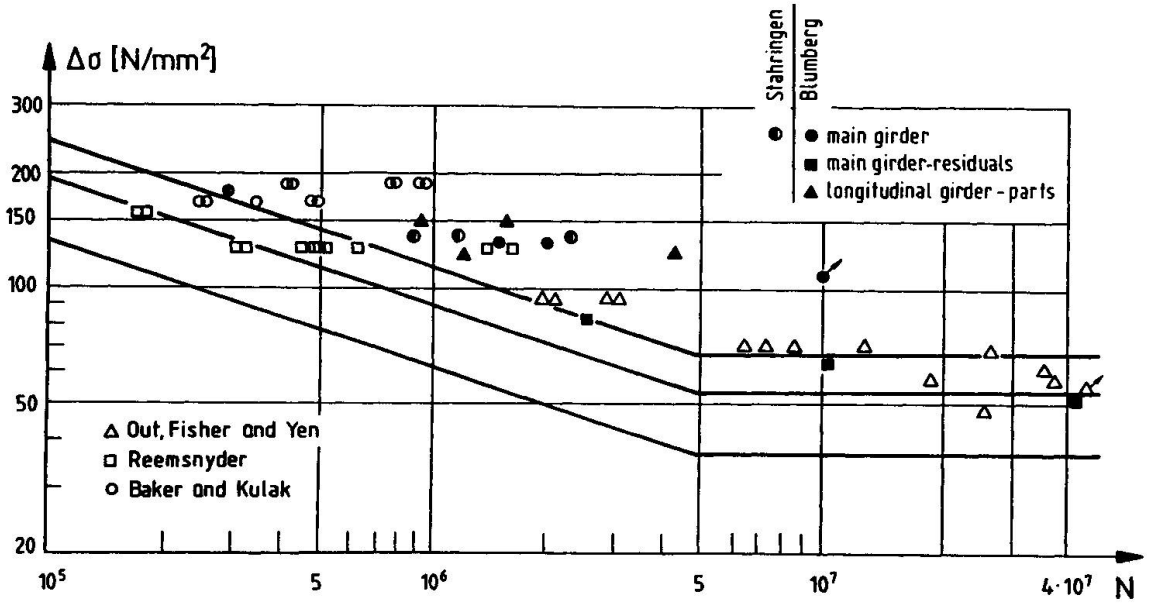

Fig. 12 Test results and data from |3|

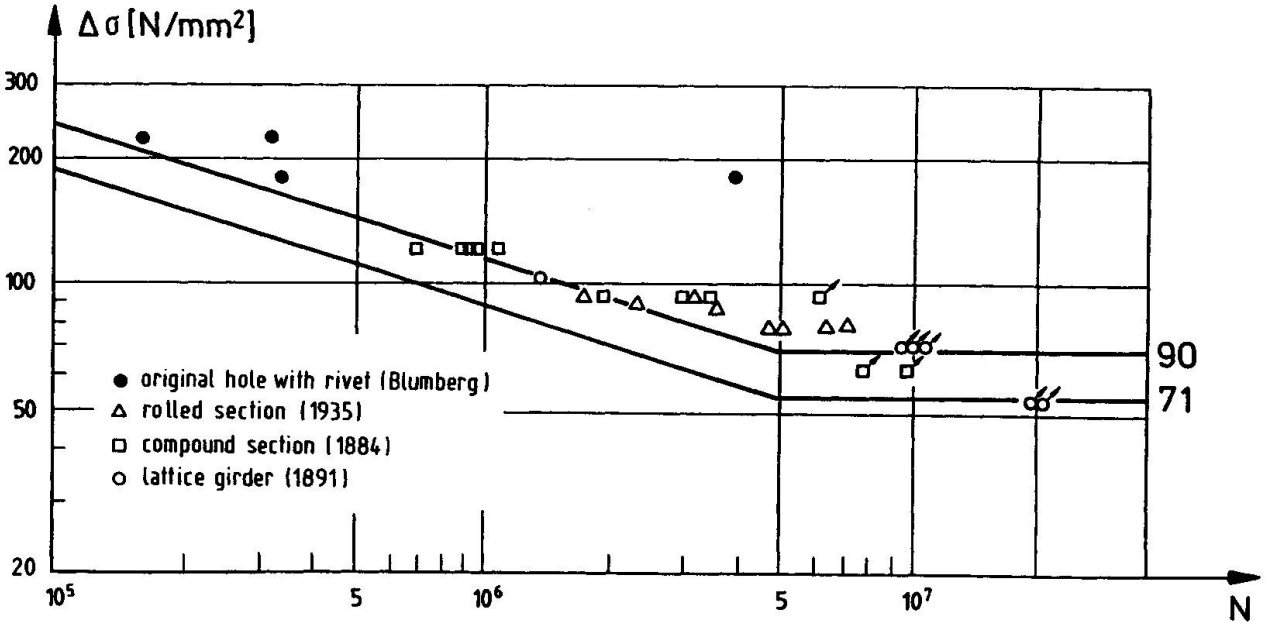

Fig. 13 Test results and data from |3|

In Figs. 14 and 15 our test results are compared to data for plain specimens dating from 1880 |3|. These diagrams are completed by data for punched and riveted specimens and for original structural components. Fig. 16 includes results of tests on structural components of the Blumberg bridge.

The annual of SFB 315 (special research program) |11| includes further comparisons particularly with the data of the draft standard DS 805 "Bewertung der Tragfähigkeit bestehender Eisenbahnbrücken" from July 1987.

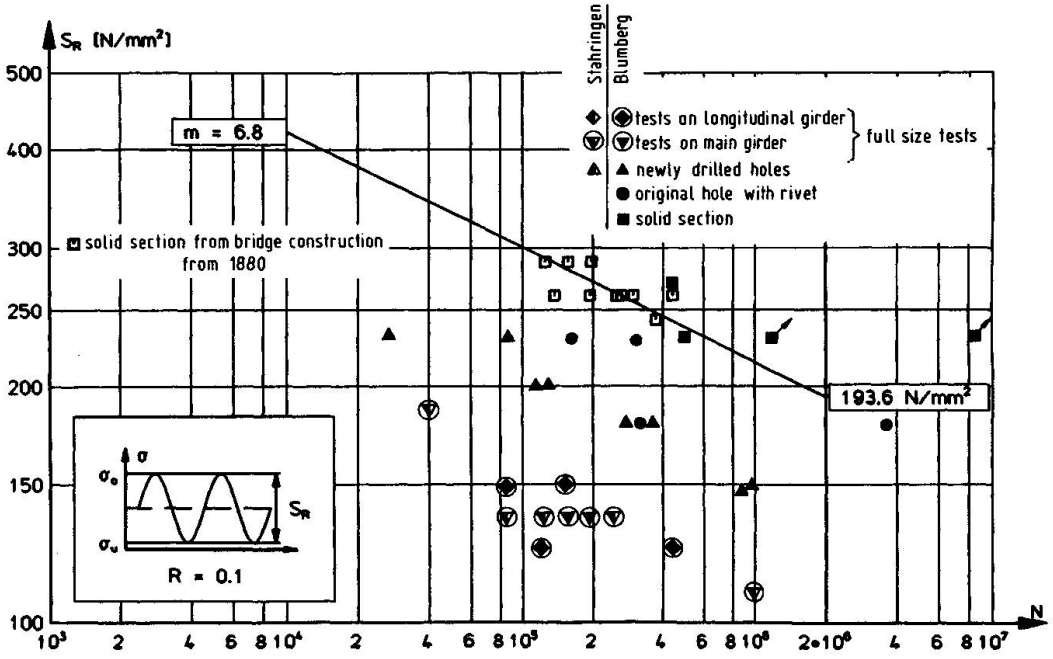

Fig. 14 Test results and data from |5|, bridges dating from 1880, plain material

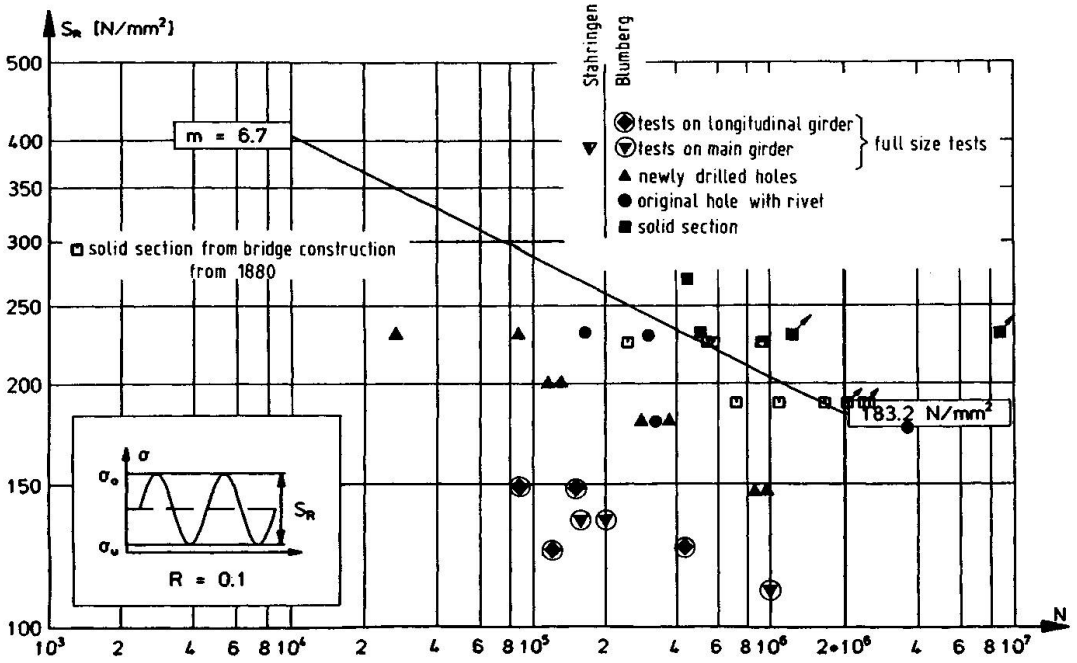

Fig. 15 Test results and data from |5|, bridges dating from 1880, plain material prestressed by 290 N/mm² and 10^5 stress cycles

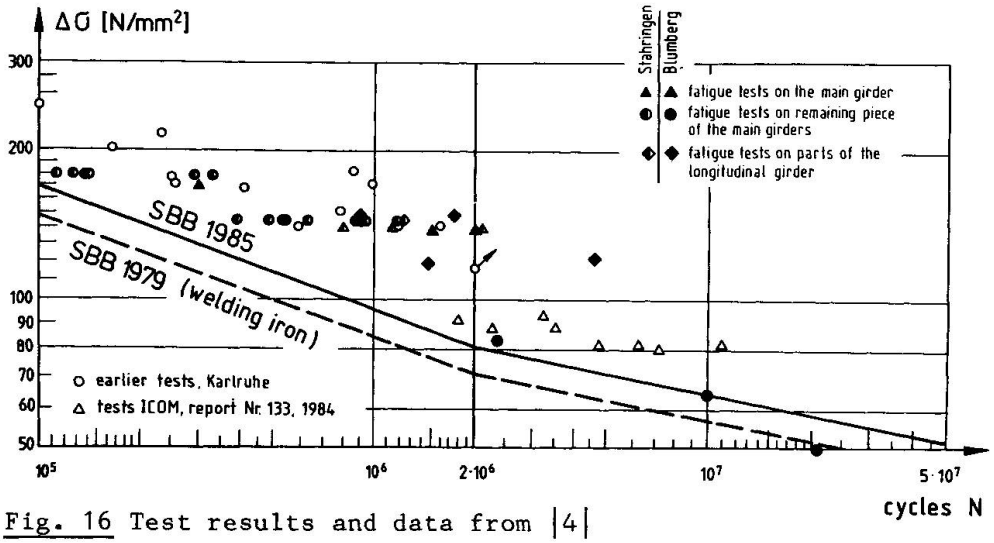

Fig. 16 Test results and data from [4]

REFERENCES

1. MANG, F., Stahl im Altbau und Wohnungsbau. Abschlußbericht zur Forschungsstudie des Landes Nordrhein-Westfalen (VBI-72.02-92/77)

2. MANG, F., STEIDL, G., BUCAK, Ö., Altstahl im Bauwesen. Schweißen und Schneiden 1985, No. 1, p. 1-5

3. BRÜHWILER, E., HIRT, M.A., Das Ermüdungsverhalten genieteter Brückenbauteile. Der Stahlbau 1987, No. 1, p. 1-8

4. HERZOG, M., Erwiderung zur Zuschrift von Tschumi, M. auf Herzog, M., Abschätzung der Restlebensdauer älterer genieteter Eisenbahnbrücken. Der Stahlbau 1986, No. 5, p. 159-160

5. BAEHRE, R., KOSTEAS, D., Einfluß der Vorbelastung auf die Restnutzungsdauer schweißeiserner Brücken. Bericht Nr. 7496 der Versuchsanstalt für Stahl, Holz und Steine der Universität Karlsruhe, Januar 1979 (not published)

6. STEINHARDT, O., Festigkeitsverhalten von Schweißeisen aus Brückenbauwerken des 19. Jahrhunderts. ETR 26 (1977), No. 6, p. 383-387

7. N.N., Unveröffentlichte Untersuchungen der Versuchsanstalt für Stahl, Holz und Steine der Universität Karlsruhe

8. STIER, W., KOSTEAS, D., GRAF, U., Ermüdungsverhalten von Brücken aus Schweißeisen. Der Stahlbau 1983, No. 5, p. 136-142

9. BUCAK, Ö., MANG, F., Untersuchungen an bestehenden Brückenbauwerken im Sinne von E-DS 805 sowie spezielle Institutsversuche an einem Originaltragwerk (Anno 1877) und an dessen Bauteilen. Festschrift Rolf Baehre, 1988. Herausgeber: O. Steinhardt und K. Möhler, Versuchsanstalt für Stahl, Holz und Steine Universität Karlsruhe

10. MANG, F., BUCAK, Ö., Theoretical and experimental investigations on railway bridges dating from 1856 to 1895. Int. Conf. on "Bridge Management", University of Surrey, March 28 - 30, 1990.

11. BAEHRE, R., WITTEMANN, K., Untersuchung der Rißausbreitung in historischen Stählen mit bruchmechanischen Methoden. Sonderforschungsbereich 315 "Erhalten historisch bedeutsamer Bauwerke", Universität Karlsruhe (to be published)

12. BUCAK, Ö., KÄPPLEIN, R., MANG, F., Ermüdungsuntersuchungen an einem Brückenbauwerk aus dem Jahre 1878. Veröffentlicht im Jahrbuch 1987 des SFB 315 "Erhalten historisch bedeutsamer Bauwerke. Verlag Ernst und Sohn, Berlin, 1987

Remaining Fatigue Strength of Corroded Steel Beams

Réserve de résistance à la fatigue de poutres en acier corrodées

Verbleibende Ermüdungsfestigkeit korrodierter Stahlträger

Pedro ALBRECHT
Professor of Civil Engineering
University of Maryland
College Park, MD, USA

Camille F. SHABSHAB
Project Engineer
Jolles Assoc., PA
Silver Spring, MD, USA

Wulin LI
Structural Engineer
Tadjer-Cohen Edelson
Silver Spring, MD, USA

William Wright
Research Structural Engineer
Federal Highway Administration
McLean, VA, USA

SUMMARY
A method is proposed for determining the remaining fatigue strength of corroded beams. The method accounts for the loss of cross-sectional area, aqueous environment, and stress concentration factors of rust pits. These three parameters can be considered separately or in any combination, depending on the type of corrosion and exposure.

RÉSUMÉ
Une méthode est proposée pour la détermination de la réserve de résistance à la fatigue de poutres corrodées. Cette méthode tient compte de la perte en section, de l'humidité ambiante, ainsi que du facteur de concentration de contrainte des piqûres de rouille. Ces trois paramètres peuvent être considérés séparément ou combinés, selon le type de corrosion et d'environnement.

ZUSAMMENFASSUNG
Vorgeschlagen wird eine Methode zur Bestimmung der verbleibenden Ermüdungsfestigkeit korrodierter Stahlträger. Berücksichtigt werden dabei der Verlust an Querschnittsfläche, die feuchte Umgebung sowie Spannungskonzentrationsfaktoren infolge der Rostkerben. Diese drei Parameter können sowohl einzeln als auch in beliebiger Kombination in Rechnung gestellt werden, je nach der Art und der Schwere der auftretenden Korrosion.

1. INTRODUCTION

Highway and railway bridges fabricated from ASTM A7, A36, and A572 steels corrode if the paint system is allowed to fail for lack of maintenance. Those fabricated from ASTM A588 atmospheric corrosion resistant (weathering) steel corrode by virtue of the steel's use in a nonpainted condition. Corroding members lose cross section and pit. The loss in cross-sectional area in the plane through a fatigue critical detail increases the nominal stress range. The pits act as stress raisers that may lead to rapid crack initiation. Precipitation, moisture, and contamination with salt from any source help to create an aqueous environment at the crack tip that accelerates crack propagation. These three effects combine to reduce the fatigue strength of corroding steel members, with the losses becoming greater the longer the exposure time.

To date, the remaining life of corroded beams has been calculated simply on the basis of the uniform corrosion loss of a member's cross section. The effect of pitting, an important factor contributing to the loss in fatigue strength, has not been included in such calculations because no information is available on the stress concentration of rust pits in structural members. the present study infers the severity of rust pits from fatigue tests of corroded A7 carbon steel [1] and A588 weathering steel beams [2] and uses this information, along with the effects of section loss and aqueous environments, to recommend a method for predicting the remaining fatigue life of corroded members.

2. EXPERIMENTS

2.1 Carbon Steel Beams

The remaining fatigue strength of the A7 rolled steel beams was determined with tests of trolley bridge stringers that were exposed to the environment for long periods of time. These stringers consisted of 4.72 m long standard beams of W 15x42 (380 mm deep and weighing 62.4 kg/m) cross section. They were removed in 1985 from a bridge carrying the Maryland Line over the Paint Branch in College Park, Maryland. The bridge was built in 1900 and abandoned in 1985. Figure 1 shows a cross section of the bridge.

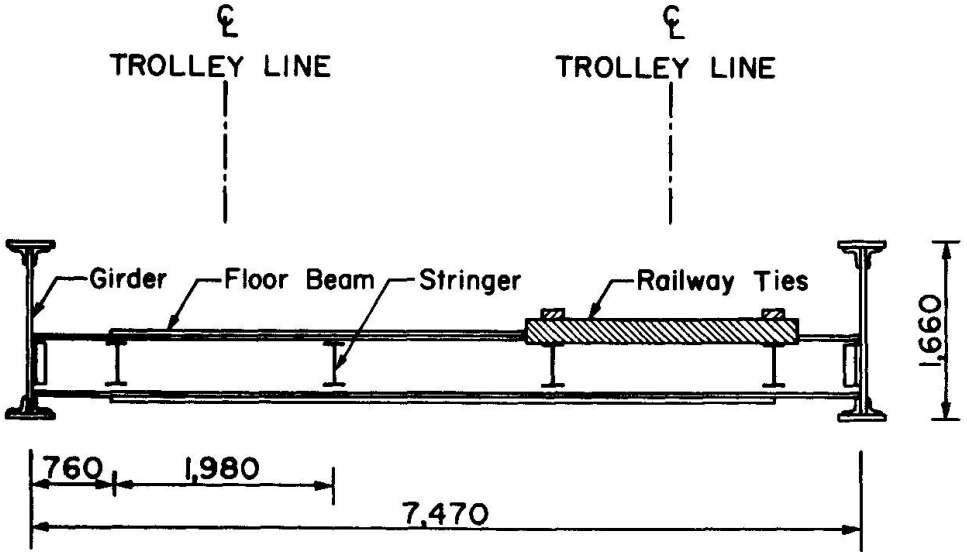

Fig. 1 Cross Section of Trolley Bridge

The trolley bridge was located in an environment of moderate corrosivity. The stringers were directly exposed to precipitation and sunshine, except for the partial shelter provided by the railway ties. The stringers corroded severely in the crevices between the railway ties and the top of the top flange, on the top of the bottom flange where debris had accumulated, and in the lower part of the web from moisture wicking up from the bottom flange by capillary action. Judging by the history of the Maryland Line, and allowing for graduate failure of the paint system, the bare steel exposure of the stringers was about 25 years.

A fatigue rating of the bridge showed that between 1900 and 1958 the stringers were subjected to about 1,900,000 cycles of 68-MPa stress range. Since the calculated mean stress range was only 41 percent of the 165-MPa fatigue limit for Category A rolled beams, the previous load history had no effect on the remaining fatigue life and was neglected. Therefore, the loss in fatigue strength observed in the test was a result of corrosion alone.

Of the 22 beam tests, nine were performed with the beams in the normal position, that is, in the same position as they were in the bridge (upside up); and 13 with the beams in the inverted position (upside down) so that the severe pits that had formed in the crevice between the top flange and the railway ties were in the tension flange during the fatigue test. In this way, the effect on fatigue could also be determined for deep pits that might occur under railway ties in a region of negative bending moment. The beams were tested in dry laboratory air.

Fatigue cracks initiated and propagated to failure in 19 beams. The tests of three beams were discontinued when no visible cracks were found after seven to ten million cycles of loading. The cracks that were found in 19 test beams initiated from the following types of defects: seven from rust pits at railway ties, eight from rust pits away from railway ties, three from imperfections at rolled-in seams, and one from an indentation at the flange tip. Eighteen beams failed from cracks that initiated in the tension flange and one in the web.

The fatigue test data for the trolley bridge stringers are compared in Fig. 2 with the allowable S-N lines for the AASHTO Category A through E details. The aforecited defects reduced the fatigue strength of the standard rolled beams from Category A for base metal to Category C for transverse stiffeners and 50 mm long attachments. The reduction in fatigue strength was greatest for rust pits at railway ties, followed by rust pits away from railway ties, and smallest for rolled-in seams and indentations.

The total reduction in fatigue strength of the trolley bridge beams can be separated into two parts. The first is attributed to the loss in cross-sectional area due to corrosion of the beam in the plane of the crack, and the second to the stress concentration effect of the rust pits. Accordingly, the fatigue notch factor (also called fatigue strength reduction factor) is equal to the product of the corrosion and pitting factors.

2.2 Weathering Steel Beams

The remaining fatigue strength of the weathering steel beams was determined with tests of 28 rolled beams of W 14x30 (360 mm deep and weighing 44.8 kg/m) cross section. The beams were placed on racks and were weathered under bold and sheltered exposures. In the former case, the beams were boldly exposed to sunshine and rain. In the latter case, the beams were covered with metal decking that simulated the sheltering of highway bridge girders by a concrete deck. Furthermore, they were sprayed three times per week during the three winter months with a three-percent sodium chloride solution to simulate the contamination of bridge girders with deicing salt. According to the steady-state corrosion rates listed in the ISO Draft Standard for Corrosion of Metals and Alloys, the bold exposure corresponded to an environment of moderate corrosivity, the bold exposure

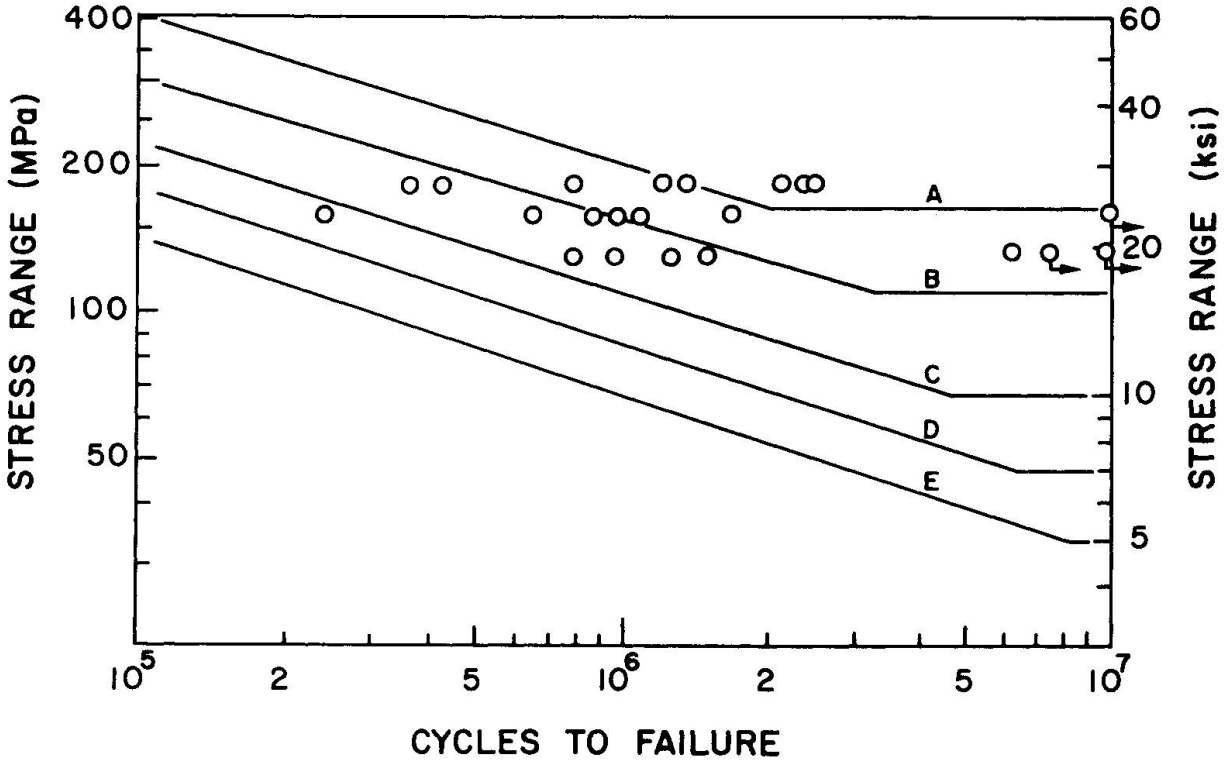

Fig. 2 Fatigue Test Data for Carbon Steel Beams

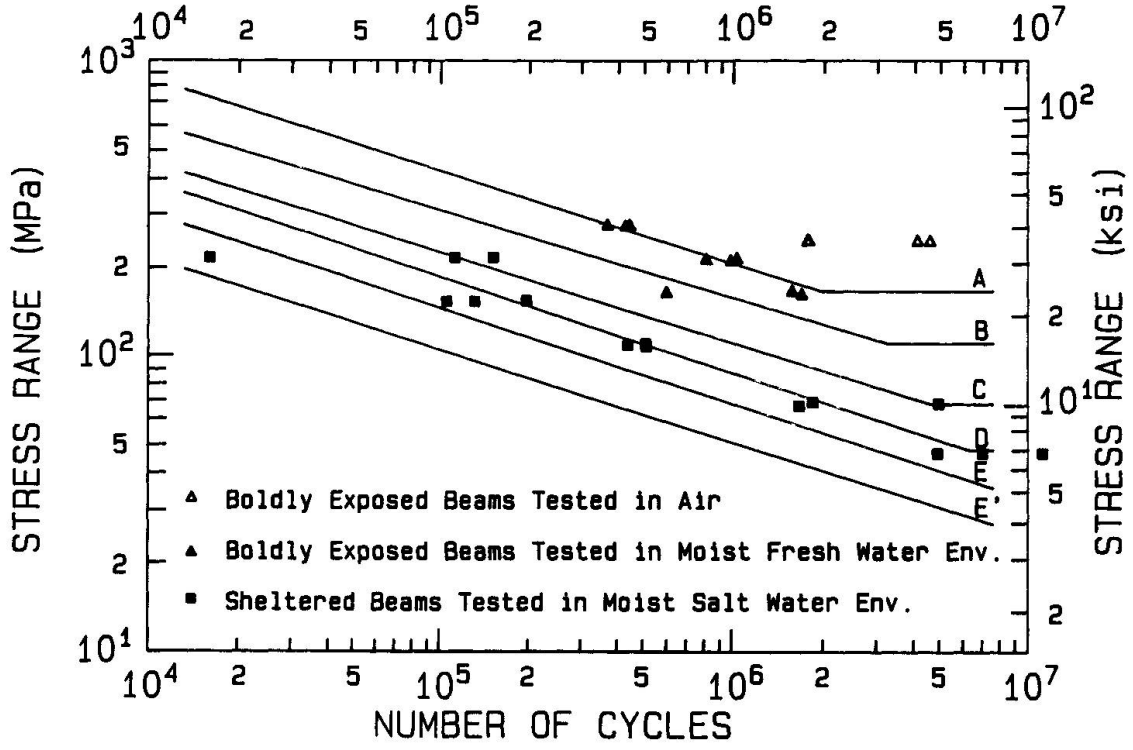

Fig. 3 Fatigue Test Data for Weathering Steel Beams

corresponded to an environment of moderate corrosivity, the sheltered exposure to an environment of very severe corrosivity. The web and flanges of the boldly exposed beams corroded to about the same degree. The bottom flange and the lower 75 mm of the web of the sheltered beams corroded much more than the top flange and upper portion of the web. The exposure time varied from five to six years.

The boldly exposed beams were fatigue tested in a moist fresh water environment, the sheltered beams in a moist salt water environment. the cyclic loads were applied at a frequency of 0.75 Hz. After an average weathering time of about 5 years, the boldly exposed beams exhibited a corrosion penetration of 0.06 mm, which is representative of bold exposure in an industrial environment. After an average weathering time of about 5.7 years, the sheltered beams exhibited a corrosion penetration of 0.32 mm for the top flange and 1.45 mm for the bottom flange. This high corrosion penetration reflects the very severe corrosivity of deicing salts.

All cracks initiated from rust pits located at the bottom of the bottom flange, except in two cases in which the pit was located on the top of the bottom flange. The deepest pit in each beam was on the average 0.34 mm for the boldly exposed beams and 2.46 mm for the sheltered beams.

The fatigue test data for the weathering steel beams are compared in Fig. 3 with the allowable S-N lines for the AASHTO Category A through E' details. As can be seen, the boldly exposed beams had Category A fatigue strength when tested in air, and B when tested in a moist fresh water environment. The sheltered beams tested in a moist salt water environment had Category E fatigue strength, with one beam failing below Category E. The loss in fatigue strength was 31 percent for the boldly exposed beams and 69 percent for the sheltered beams. The total reduction in fatigue strength exhibited by the beams tested in the aqueous environments is attributed to (a) the loss in cross-sectional area due to corrosion in plane of crack, (b) the aqueous test environment, and (c) the stress concentration effect of the rust pits. Accordingly, the fatigue notch factor of a bare exposed weathering steel beam can be expressed as the product of the corrosion, environment, and pitting factors.

3. METHOD OF ANALYSIS

3.1 General Equations

The total reduction in fatigue strength of a corroded beam is the vertical distance in Fig. 4 between the solid data point D for that beam and point A on the mean S-N line for Category A rolled beams given by

$$\log N = b - m \log f_r \qquad (1)$$

where N = number of cycles to failure, f_r = stress range based on dimensions of beam before weathering, m = 3.178, and b = 13.785 for f_r in units of MPa [3]. The following three factors contribute to that reduction: (1) loss in cross-sectional area due to corrosion of beam in plane of crack, (2) stress cycling in aqueous environment, and (3) stress concentration effect of rust pits.

The total reduction in fatigue strength can be expressed in terms of the fatigue notch factor for the corroded beam

$$K_{fc} = \frac{f_{r,A}}{f_r} \qquad (2)$$

where $f_{r,A}$ = mean stress range for AASHTO Category A rolled beams obtained by substituting the fatigue life of the test beam, N, into Eq. 1.

The total reduction in fatigue strength can then be separated into the three factors

$$K_{fc} = K_c \, K_e \, K_p \tag{3}$$

where K_c = strength reduction factor attributed to loss in cross-sectional area due to corrosion of beam in plane of crack, K_e = strength reduction factor attributed to effect of aqueous environment, and K_p = strength reduction factor attributed to stress concentration effect of rust pits.

The terms K_c, K_e, and K_p are hereafter referred to as the corrosion factor, environment, and pitting factors, respectively. Their logarithms are equal to the distances CD, BC, and AB shown in Fig. 4. The corrosion factor is calculated from

$$K_c = \frac{f_{r,c}}{f_r} \tag{4}$$

where $f_{r,c}$ = stress range at bottom flange of corroded section in plane ofcrack.The test environment factor is related to the ratio of the crack growth rates in aqueous and air environments.

$$K_e = \left\{ \frac{(\frac{da}{dN})_{aq.}}{(\frac{da}{dN})_{air}} \right\}^{1/n} \tag{5}$$

where n = slope constant in plot of crack growth rate versus range of stress intensity factor.

Knowing K_c, K_e, and K_{fc} for a given set of fatigue test data, Eq. 3 can then be solved for the pitting factor, K_p.

$$K_p = \frac{K_{fc}}{K_c \, K_e} \tag{6}$$

The calculation of the values K_c, K_e, and K_{fc} for the beams tested in the present study are described in the following.

3.2 Corrosion Factor

The stress range, f_r, to which a beam was subjected is given by

$$f_r = \frac{M_r \, y}{I} = \frac{M_r}{S} \tag{7}$$

where M_r = moment range; and the properties of the section before corrosion are y = distance from neutral axis to extreme tension fiber, I = moment of inertia, and S = section modulus.

Figs. 5 and 6 show with solid lines the corroded section in the plane of the crack and with dashed lines the non-corroded section. The section loss in the plane of the crack affects the stress range in two ways: (1) the loss in cross sectional area reduces the moment of inertia, and (2) the unequal thickness losses of the top and bottom flanges shift the neutral axis of the section. The stress range at the bottom flange of the corroded section in the plane of the crack is given by

$$f_{r,c} = \frac{M_r\, y_c}{I_c} = \frac{M_r}{S_c} \tag{8}$$

where, for the corroded section, y_c = distance from neutral axis to extreme tension fiber, and I_c = moment of inertia in plane of crack, and S_c = section modulus. Substituting Eqs. 7 and 8 into Eq. 4 gives the following expression for the corrosion factor:

$$K_c = \frac{S}{S_c} \tag{9}$$

The cross-sectional properties needed to calculate the corrosion factor for a standard beam section (Fig. 5) are the moment of inertia of the noncorroded section

$$I = \frac{1}{12}\left\{ b_f d^3 - \frac{(b_f - t_w)}{8\,(m-n)}\left[(d-2n)^4 - (d-2m)^4\right]\right\} \tag{10}$$

the position of the centroidal axis of the corroded section

$$y_c = \frac{A\frac{d}{2} - \left[\Delta A_b \frac{m+n}{4} + \Delta A_w \frac{d}{2} + \Delta A_t \left(d - \frac{m+n}{4}\right)\right]}{A - (\Delta A_b + \Delta A_w + \Delta A_t)} - C_b \tag{11}$$

and the moment of inertia of the corroded section

$$I_c = I + A\left(y_c + C_b - \frac{d}{2}\right)^2 - \Delta A_b \left(y_c + C_b - \frac{m+n}{4}\right)^2 - \frac{2C_w d^3}{12}$$

$$- \Delta A_w \left(y_c + C_b - \frac{d}{2}\right)^2 - \Delta A_t \left(d - y_c - C_b - \frac{m+n}{4}\right)^2\Big] \tag{12}$$

where

$$\Delta A_b = 2C_b(b_f - 2C_w) \qquad \Delta A_w = 2C_w d \qquad \Delta A_t = 2C_t(b_f - 2C_w) \tag{13}$$

For the wide flange section, the moment of inertia is given by (Fig. 6)

$$I = \frac{b_f d^3 - (b_f - t_w)\,(d - 2t_f)^3}{12} \tag{14}$$

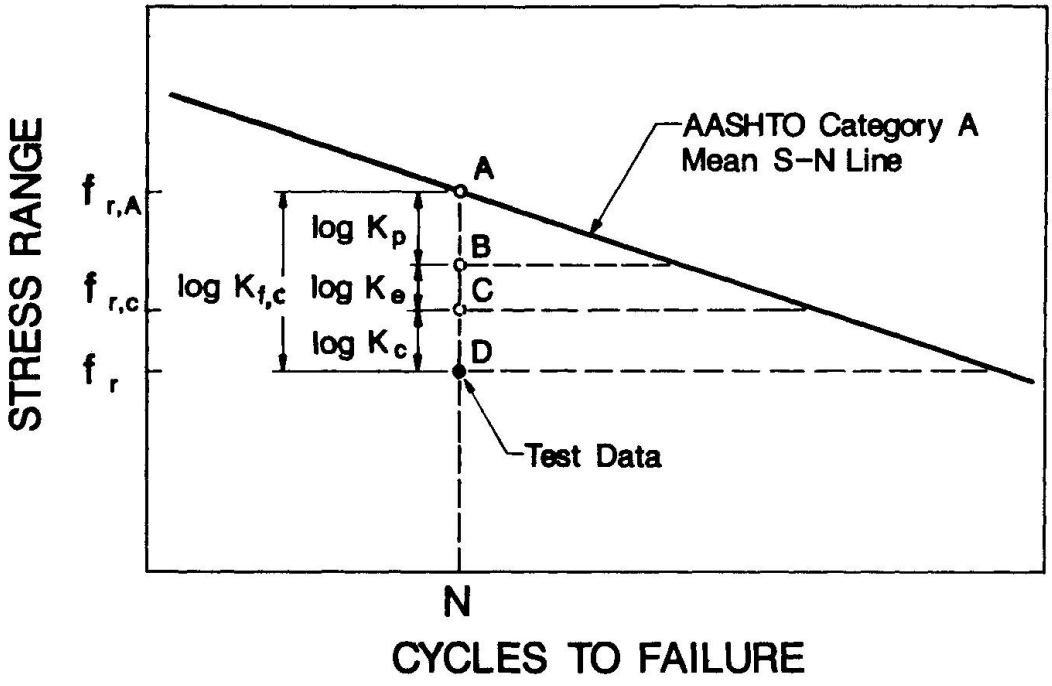

Fig. 4 Illustration of Fatigue Strength Reduction Factors

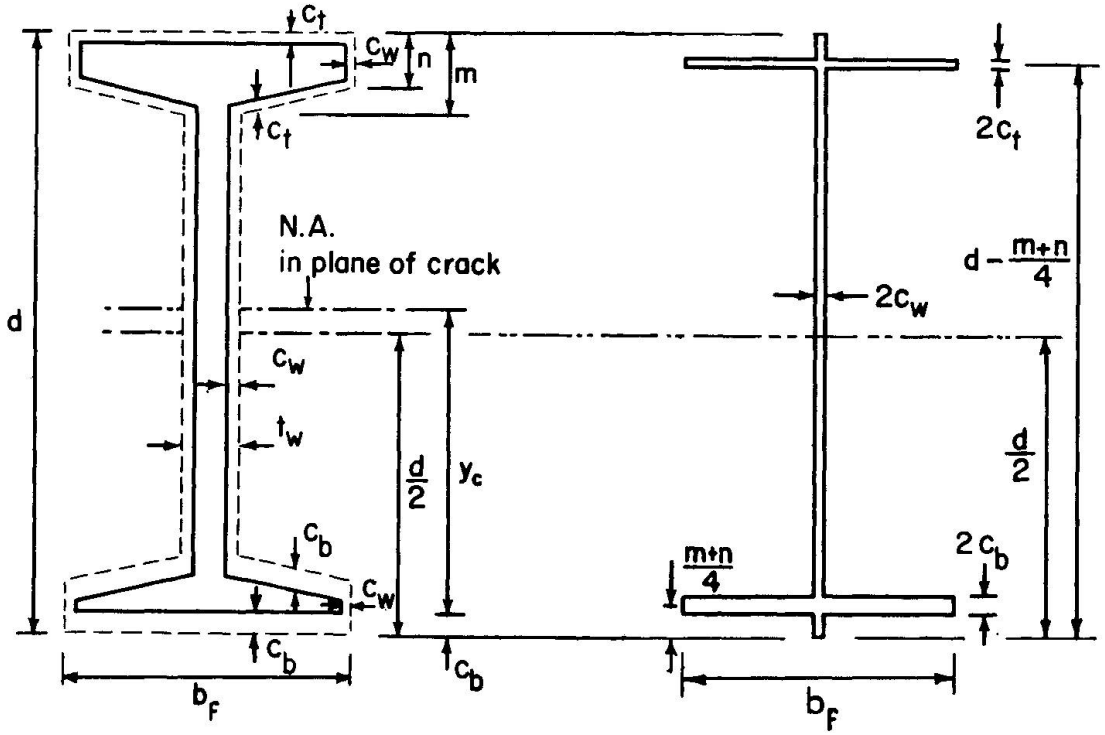

Fig. 5 Standard Beam with Noncorroded and Corroded Sections on left, Section Loss on Right

while the position of the centroidal axis and the moment of inertia of the corroded section are obtained by substituting $m+n = 2t_f$ in Eqs. 11 through 13. All dimensions are defined in Figs. 5 and 6.

The corrosion factor was calculated individually for each beam. It was on the average $K_c = 1.09$ for the carbon steel beams, 1.02 for the boldly exposed weathering steel beams, and 1.37 for the sheltered weathering steel beams.

3.3 Environment Factor

The crack growth rate for mild and high-strength low-alloy (HSLA) steels stress cycled in air differs significantly from that for the same steels stress cycled in an aqueous environment. The crack growth rate is, in air [5]:

$$(\frac{da}{dN})_{air} = 1.537 \times 10^{-12} \ (\Delta K_{eff})^{3.344} \tag{15}$$

and in aqueous environments

$$(\frac{da}{dN})_{aq.} = 4.161 \times 10^{-12} \ (\Delta K_{eff})^{3.279} \tag{16}$$

where da/dN = crack growth rate in m/cycle and ΔK_{eff} = stress intensity factor in $MPa\sqrt{m}$.

Eqs. 15 and 16 appear as nearly parallel lines in a base-10 logarithmic plot of da/dN versus ΔK_{eff}. Hence, the effect of the aqueous environment on the crack growth rate is uniform over the range of data.

The fatigue life reduction factor due to the aqueous environment is the ratio of the crack growth rates. The fatigue strength reduction factor is then given by the n-th root of the fatigue life reduction factor (Eq. 5) where $n = 3.3$ is the average exponent in Eqs. 15 and 16. At the lowest stress intensity factor range [$\Delta K_{eff} = 14.8$ $MPa\sqrt{m}$ (13.5 $ksi\sqrt{in.}$)] at which corrosion fatigue crack growth rates were measured, cracks grew a factor of 2.3 faster in aqueous environments than in air [5]. Hence, the environment factor is on the average $K_e = (2.3)^{1/3.3} = 1.3$ for the wide flange beams tested in aqueous environments.

3.4 Pitting Factor

Knowing the values of K_{fc}, K_c, and K_e, the strength reduction factor attributed to the stress concentration effect of the rust pits, K_p, was then calculated with Eq. 6. The value of K_p for the carbon and weathering steel beams were plotted in Figs. 7 and 8 against the maximum measured pit depth in the plane of the crack. The mean regression lines going through the point with coordinates $d_p = 0$ and $K_p = 1.0$ are, for the carbon steel beams:

$$K_p = 1.0 + 0.22 \ d_p \tag{17}$$

and for the weathering steel beams

$$K_p = 1.0 + 0.40 \ d_p \tag{18}$$

where d_p = pit depth in units of millimeter. The depth was used in the present study as the simplest measure of the severity of the stress concentration factor caused by a pit. Other measures also affect the stress concentration such as the

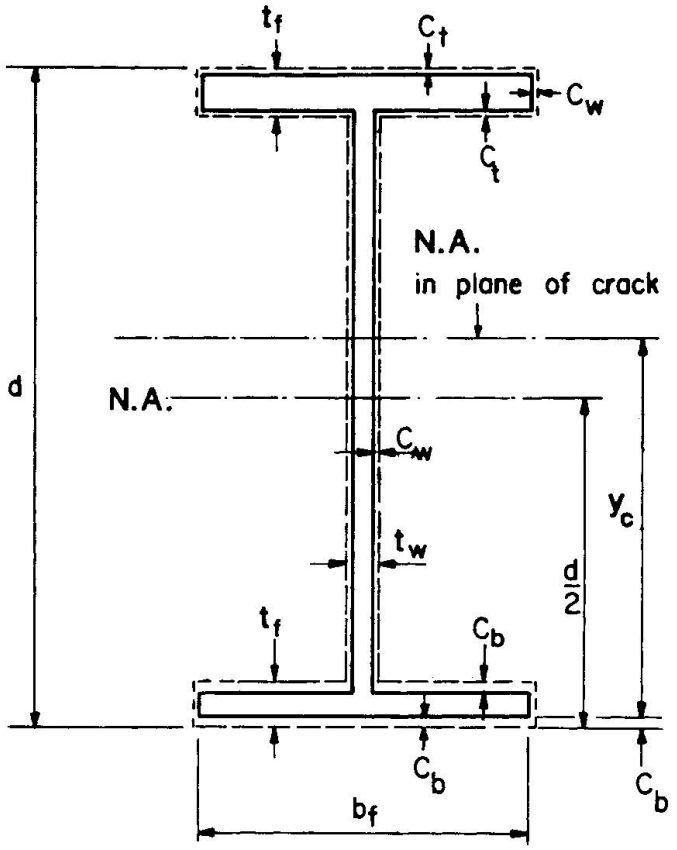

Fig. 6 Wide Flange Beam with Noncorroded and Corroded Sections

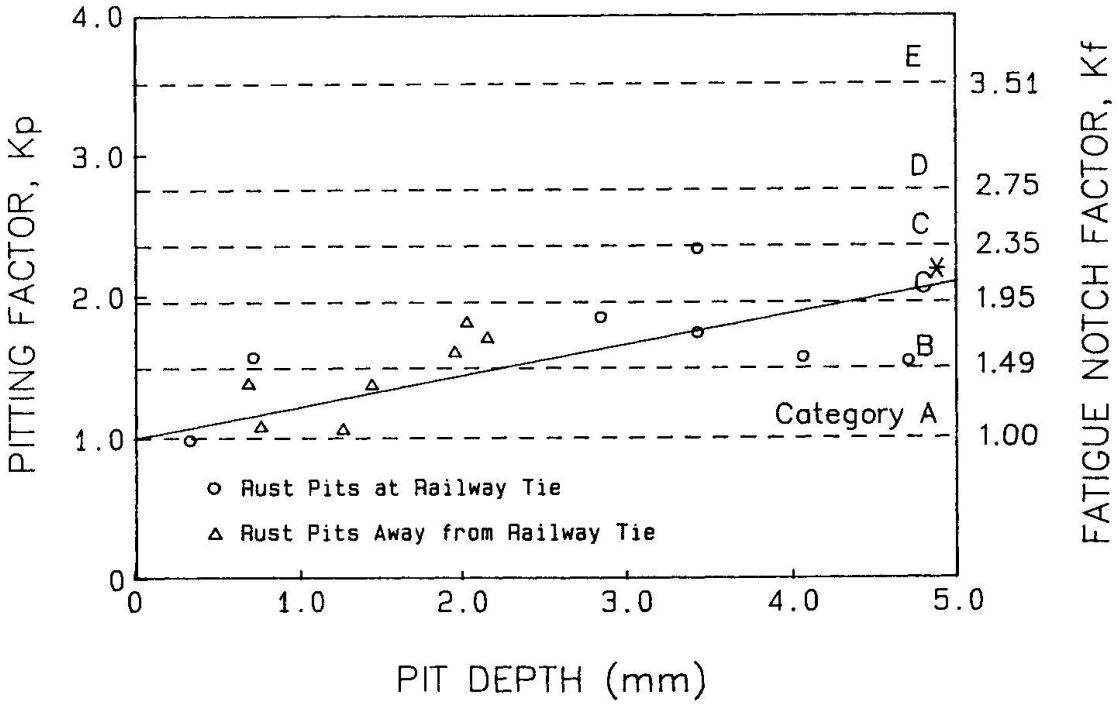

Fig. 7 Pitting Factor for Carbon Steel Beams

slope of the pit walls and the depth-to-diameter ratio. Including them could lead to more accurate results if each pit were separate from the others. However, this was rarely the case.

The pitting factors are compared with the fatigue notch factors, K_f, of the mean S-N lines for Category A--base metal, B--welded beams, C*--transverse stiffeners, C--50 mm long attachments, D--100 mm long attachments, and E--partial length cover plates. The values of K_f are shown as horizontal lines in Figs. 7 and 8. The following conclusions can be drawn from these results. First, the pitting factor increased on the average with pit depth. Second, for equal depths, a pit induced a much higher stress concentration in a weathering steel beam than in a carbon steel beam. Indeed, the pits in the weathering steel beams were found to have steeper walls and at times flat bottoms, while those in the carbon steel beams had a more rounded profile. Third, pitting reduced the fatigue strength more than section loss, $K_p > K_c$.

As an example of the severity of the rust pits in weathering steel beams, substituting the fatigue notch factors listed on the right vertical axis of Fig. 8 into Eq. 17 in place of K_p and solving for d_p, one finds that pit depths of d_p = 1.2, 2.4, 3.4, and 4.4 mm, respectively, reduced the fatigue strength of the weathering steel beams on the average to the mean fatigue strength of Category B welded beams, Category C* transverse stiffeners, Category C 50-mm attachments, and Category D 100-mm attachments.

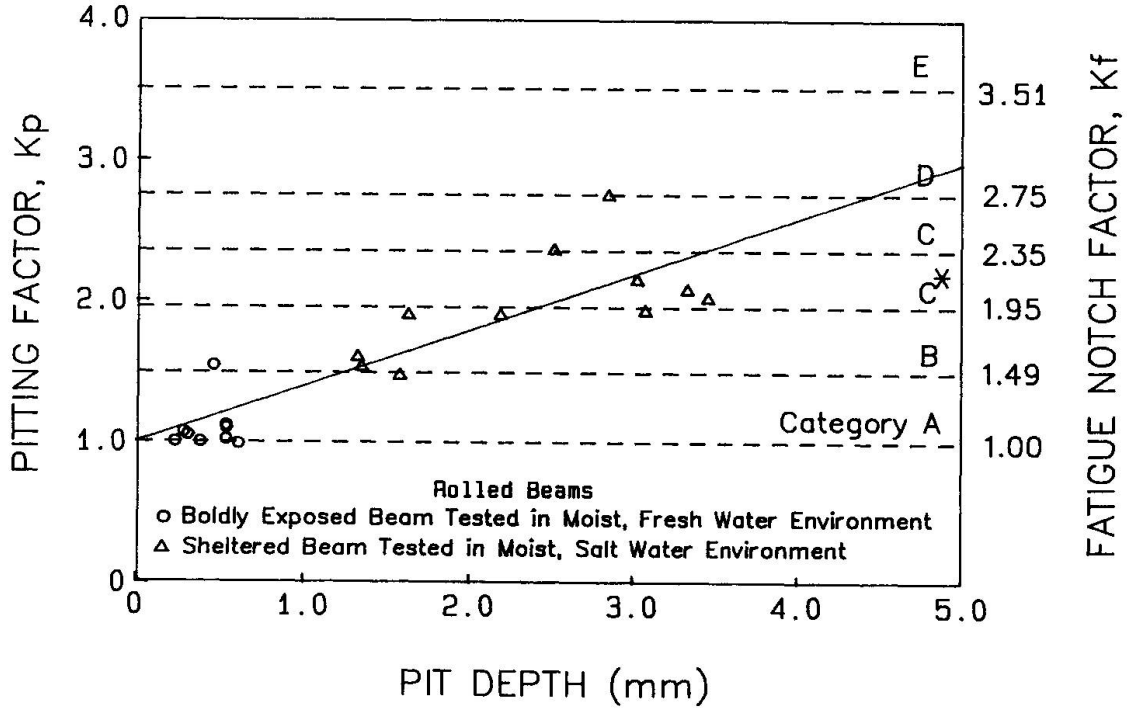

Fig. 8 Pitting Factor for A588 Weathering Steel Beam

4. DESIGN RECOMMENDATIONS FOR EXISTING STRUCTURES

The remaining fatigue life of corroded rolled beams in existing structures may be calculated following the procedure outlined below.

1. Calculate with Eq. 7 the stress range, f_r, at the critical section of the non-corroded beam.

2. Measure the corrosion penetration using an electrically powered disk grinder and an ultrasonic thickness gage as follows [6,7,8]:

   - Grind a 25 mm wide strip across one surface of the bottom flange, web, and top flange until bare metal is exposed on the highest points of the corroded surfaces, leaving the depressions filled with dense oxide. Approximately 30 percent of the so-ground surface should have a metallic appearance.

   - Measure the thickness of the web and flanges with the ultrasonic thickness gage at 20-mm intervals along the ground strips. At each measurement point, move the ultrasonic probe in an area of 20-mm diameter and retain the smallest reading. This peak-to-valley reading gives a good estimate of the plate thickness.

   - Average the measured thicknesses of the web and each flange separately.

   - Subtract the measured plate thicknesses from the original thicknesses of the members specified on the as-built drawings. Divide the difference by two to obtain the uniform corrosion penetration per side of the web and each flange plate.

3. Using the Eqs. 10 through 14 listed in Section 3.2, calculate the cross-sectional properties of the beam before and after corrosion, the latter being based on the corrosion penetration values measured in Step 2.

4. Calculate the corrosion factor, K_c, with Eq. 9.

5. Continuing the process described in Step 2, measure the pit depth as follows:

   - Continue to grind the strips until only traces of oxide remain.

   - Measure again the thickness with the ultrasonic thickness gage and retain the smallest reading. This represents the valley-to-valley thickness.

   - Substract the valley-to-valley thickness from the peak-to-valley thickiness measured in Step 2 to obtain the pit depth.

   Alternatively, pit depths can be measured with a depth gage after blast cleaning the non-ground surface to bare metal.

6. Calculate the pitting factor, K_p, with Eq. 17 for carbon steel beams and Eq. 18 for weathering steel beams, using the pit depth measured in Step 5.

7. If the structure will remain exposed in a bare condition, as may be the case for weathering steel, assume a value for the environment factor, say, $K_e = 1.3$. If the structure is to be painted, set $K_e = 1.0$.

8. Calculate the allowable fatigue life as

$$N_d = \frac{10^{b-2s}}{(K_c K_e K_p f_r)^m} \tag{19}$$

where b, m, and s are the intercept, slope, and standard deviation of the mean S-N line for Category A base metal (see for example Table 1 of Ref. 4).

9. Estimate the number of stress range cycles, N_{used}, that were applied on the structure to date.

10. Calculate the remaining number of stress range cycles, $N_{rem.}$, that may be applied on the structure until it reaches the allowable fatigue life.

$$N_{rem.} = N_d - N_{used} \tag{20}$$

5. APPLICATION TO OTHER TYPES OF DETAILS

The recommendations for calculating the remaining fatigue life of corroded rolled beams, outlined in Section 4, can also be applied to other types of details. Two cases are possible, depending on whether the notch effect of a pit is smaller or greater than that of a given type of detail. If the pitting factor is smaller than the fatigue notch factor for the noncorroded detail, $K_p < K_f$, the fatigue notch factor for the corroded detail is given by

$$K_{fc} = K_c K_e K_f \tag{21}$$

If, on the other hand, $K_p > K_f$, then

$$K_{fc} = K_c K_e K_p \tag{22}$$

The authors have verified the extension of this method to two other types of details that were exposed in a sheltered condition for 4.3 to 6.5 years and then fatigue tested in a moist salt water environment. These details consisted of Category B welded beams and Category E rolled beams with partial-length cover plates fabricated from A588 weathering steel [2].

Like the Category A rolled beams of A588 steel whose data were presented in this paper, the fatigue strength of the corroded Category B welded beams was reduced to that of Category E, meaning that $K_p > K_f$. Furthermore, the equation relating pit depth to pitting factor for the welded beams was about the same as the corresponding Eq. 18 for the rolled beams.

Finally, sheltered exposure and stress cycling in a moist salt water environment did not significantly affect the fatigue strength of the Category E coverplated beams of A588 steel, meaning that $K_p < K_f$.

So, Eq. 21 should be used for the Category B welded beams and Eq. 22 for the Category E welded beams. If at the time the analysis is performed it is decided

to paint the weathering steel beams, then a value of $K_e = 1.0$ should be chosen in the calculation of remaining life.

REFERENCES

1. Albrecht, P., and Xu, G., Fatigue Strength of Long-Term Weathered Rolled Beams. Department of Civil Engineering, University of Maryland, College Park, Maryland, March, 1988.

2. Albrecht, P., et al., Fatigue Strength of Weathered A588 Steel Beams. Report No. FHWA/MD-89/01, Department of Civil Engineering, University of Maryland, College Park, Maryland, 1990.

3. Fisher, J.W., Frank, K.H., Hirt, M.A., and McNamee, B.M., Effect of Weldments on the Fatigue Strength of Steel Beams. NCHRP Report 102, TransportationResearch Board, National Research Council, Washington, D.C., 1970.

4. Albrecht, P., and Simon, S., Fatigue Notch Factors for Structural Details. Journal of the Structural Division, ASCE, Vol. 197, No. ST7, July, 1981, pp. 1279-1296.

5. Yazdani, N. and Albrecht P., Crack Growth Rates of Structural Steels in Air and Aqueous Environments. Journal of Engineering Fracture Mechanics, Vol. 32, No. 6, 1989, pp. 997-1007.

6. Albrecht, P., et al., Guidelines for the Use of Weathering Steel in Bridges. NCHRP Report 314, Transportation Research Board, National Research Council, June, 1989.

7. McCrum, R.L., Arnold, C.J., and Dexter, R.P., Current Status Report-Effects of Corrosion on Unpainted Weathering Steel Bridges. Report No. R-1255, Michigan Department of Transportation, Lansing, Michigan, February, 1985.

8. Standard Practice for Measuring Thickness by Manual Ultrasonic Pulse-Echo Contact Method. ASTM Designation E797, American Society for Testing and Materials, Vol. 03.03, Philadelphia, Pennsylvania, 1983.

Toughness and Fracture Behaviour of Obsolete Wrought Bridge Steel

Résistance et comportement à la rupture d'anciens ponts en fer puddlé

Bruchzähigkeit und Bruchverhalten von Material alter Schweisseisen-Brücken

Hans-Jakob SCHINDLER
Dr. sc. techn.
EMPA
Dübendorf, Switzerland

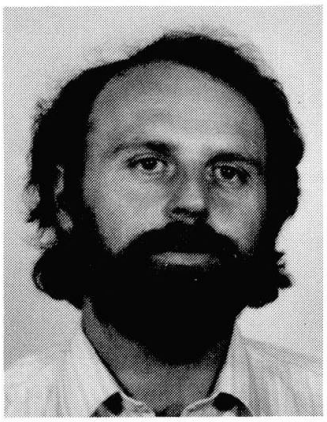

Hans-Jakob Schindler, born 1953, received his civil engineering and doctoral degree at ETH (Swiss Federal Institute of Technology) Zurich. Afterwards, he joined a consulting engineering firm, working in the field of structural dynamics. Now at EMPA (Swiss Federal Laboratories for Materials Testing and Research), he is dealing principally with research into fracture mechanics applications.

Ulrich MORF
Dr. sc. techn.
EMPA
Dübendorf, Switzerland

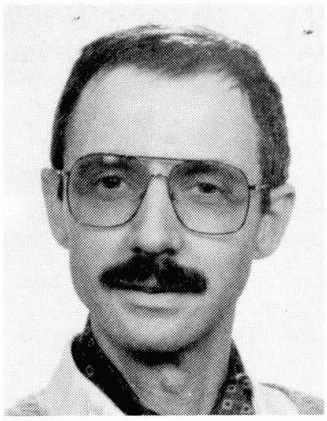

Ulrich Morf, born 1942, obtained his engineering and doctoral degree at ETH (Swiss Federal Institute of Technology) Zurich. Since 1971, after being a design engineer in a steel construction firm, he has been head of the Department Metals Technology and Structures of EMPA (Swiss Federal Laboratories for Materials Testing and Research).

SUMMARY
In old bridges the presence of fatigue cracks or sharp notches can hardly be excluded. Thus the question arises as to how the material behaves in presence of such defects. In the present paper, it is shown, using a case of a bridge made of wrought iron, how fracture mechanics enables some quantitative predictions concerning crack-sensitivity to be carried out.

RÉSUMÉ
Dans les vieux ponts en acier, on ne peut pas exclure complètement l'existence de défauts tels que des fissures de fatigue et des entailles. Il se pose alors la question de la sensibilité du matériau à de tels défauts. Dans cet article, on démontre pour le cas d'un pont en fer puddlé que la mécanique de la rupture fournit des indications quantitatives sur le comportement des zones fissurées.

ZUSAMMENFASSUNG
In alten Brücken kann das Vorhandensein von Ermüdungsrissen oder scharfkantigen Kerben selten ausgeschlossen werden. Es stellt sich deshalb die Frage nach der Fehlerempfindlichkeit des Materials. Im vorliegenden Bericht wird am Beispiel einer Brücke aus Schweisseisen gezeigt, wie sich mit Hilfe der Bruchmechanik einige quantitative Angaben zur Rissempfindlichkeit machen lassen.

1. INTRODUCTION

In Switzerland there is a fairly large number of approximately 100 year old bridges which are still in service. Most of them are riveted framework structures made of wrought steel. In order to be able to deal with problems like safety, reliability or remaining life of such structures it is important to know as much as possible about the actual mechanical and toughness properties of these materials.

Traditional elastic design of structural elements is based on classic stress analysis ("elastic" design) or on calculation of the plastic collapse load ("plastic" design). In the latter case the material is supposed to be able to deform plastically. In [1] a flow chart a systematic demonstration of the safety of a structure is presented. Based on ideas given in [2] it is suggested to proceed in three steps: classical design, failure analysis and failure assessment under extreme conditions at the end of the service life. Within such a safety analysis for obsolete steels material testing on the basis of fracture mechanics or related tests are of great importance for the designer.

In general there is not only the global strength and stability of the structure to be investigated, but also local problems like fatigue crack growth and residual strength of cracked components. Since there is only little known about fatigue crack growth, one can hardly exclude the possibility of cracks in critical components, typically e.g. a crack emanating from a rivet hole hidden by the head of the rivet. From the relatively poor properties related to ductility and toughness, like Charpy fracture energy and reduction in area, one must conclude a relatively low toughness [3, 4]. Thus there is a strong need to know as much as possible about the crack–sensitivity of the material, i.e. the behaviour of the material in presence of cracks or crack–like defects.

The adequate means for treating these kind of problems is the theory of fracture mechanics. Concerning wrought iron there is an apparent lack of knowledge in this field. It is the topic of the present investigation to get more insight in the fracture behaviour and fracture mechanisms of wrought iron in the presence of a sharp crack. First it is shown, how the fracture toughness of wrought iron was determined and by which parameters it is influenced, and how the material properties can be used to predict the fracture behaviour of structural elements.

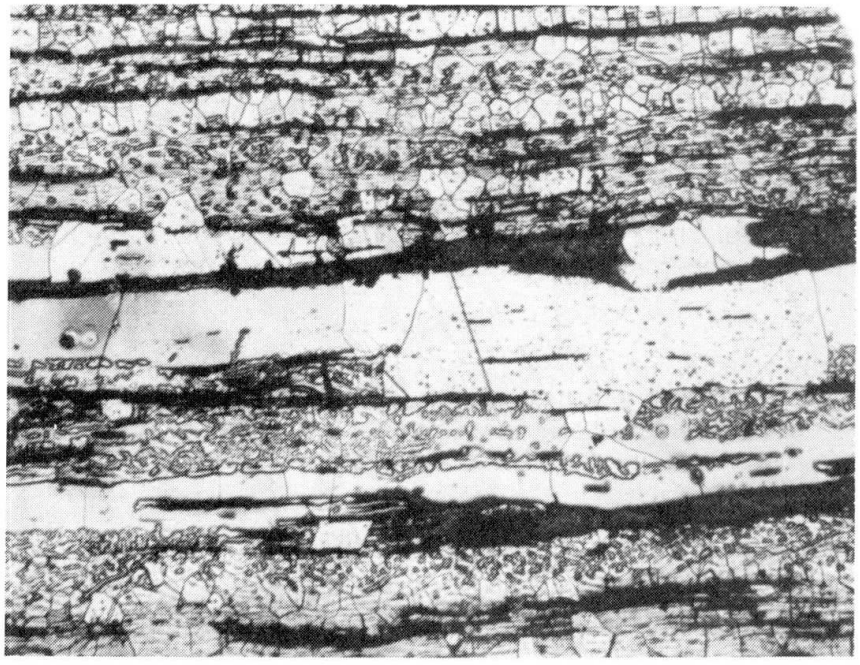

Fig. 1: Microstructure of wrought iron (magn. 50x)

2. MATERIAL

The characteristics of wrought iron is its layered structure, which is a result from the manufacturing process. It consists of sheet shaped layers of recristallized ferrite and of nonmetallic inclusions (Fig.1). Because of the anisotropy of the material several loading directions and crack orientations have to be differentiated in material testing. The present investigation is restricted to loading in axial direction and crack–extension in–plane (with respect to the material layers) and out–of–plane (crack type A resp. B, see Fig. 2). This structure can be clearly seen on the fracture surfaces of broken specimens, which exhibit a "wood–like" topography.

The mechanical properties in axial direction of the material used in the present investigation are given in Tab. 1. Concerning the yield stress and the ultimate tensile strength the material is comparable to an ordinary structural steel. The properties related to ductility and toughness, like elongation, uniform strain and reduction in area at fracture, are apparently lower than in the case of ordinary steel. The charpy impact energy is extremely low. Unlike ordinary structural steel there is only a minor increase of impact energy within the transition region. The fracture energy remains at relatively low values even for full ductile fracture. Thus the material appears to be considerably more brittle than common structural steel of today.

The relatively low uniform strain should be taken into account especially in cases of additional loads, short–term overloads, erection procedures, etc. Any modification which causes or requires plastic redistribution of stresses or plastic settlements should be avoided.

In other loading directions the ductility–related properties are even worse. This has to be accounted for e.g. in the case of repair. Any heat effect due to preheating, welding or oxy–arc cutting may transform the metallurgic structure such that the (favorable) anisotropy is destroyed. Since the content of sulfur, phosphorus and other impurities is relatively high, new brittle alloys may be formed by remelting. Therefore repair by welding should be omitted.

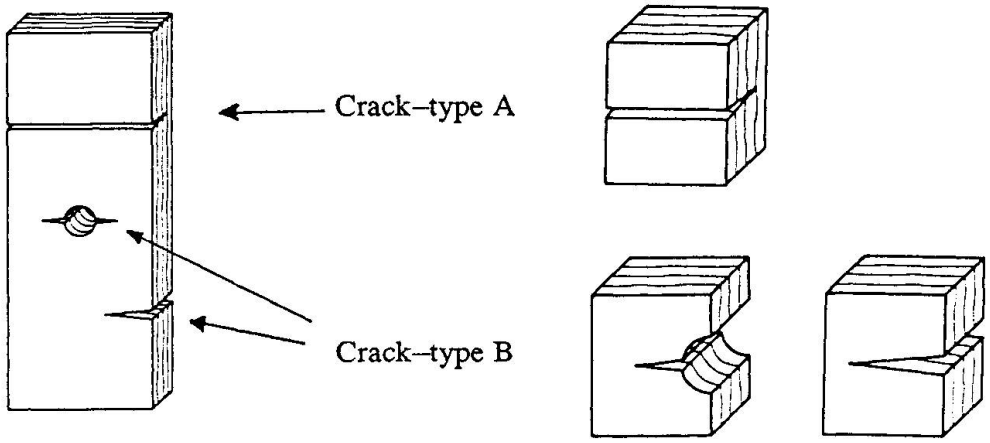

Fig. 2: Definition of crack–type A resp. B.

Yield stress [MPa]	Ultimate strength [MPa]	Elongation at fracture [%]	Uniform strain [%]	Red. in area [%]	Charpy impact energy (cr.typeA) [J]	
					RT	100°C
241	371	21	0 - 16	31	10 - 18	44

Tab. 1: Material properties of the investigated wrought iron

3.1. MATERIAL TESTING ON THE BASIS OF FRACTURE MECHANICS

3.1. General

In order to quantify the crack–sensitivity of the material and to predict the fracture behaviour of a structural component in presence of a crack or similar stress–raisers the theory of fracture mechanics is the adequate means. For an introduction in this field we refer to [5]. There are several parameters to characterize toughness in the sense of fracture mechanics, the most widely used being the critical stress intensity factor K_{1c}, the so–called plane strain fracture toughness, a factor which characterizes the resistance of the material against crack–growth. Although it looses its physical significance in the case of cracks in mild steel like wrought iron and of relatively thin–walled structural components like the typical structural members considered in the present investigation, it still is useful as a material property and also in order to perform a failure assessment analysis (e.g by applying the so–called R6–Method, see later in this article).

3.2. Determination of K_{Ic}

One of the difficulties in applying fracture mechanics to mild steels is the experimental determination of K_{1c}. Since large plastic straining occurs prior to forced crack growth, the underlying assumptions according to the theory of linear elastic fracture mechanics are no longer fulfilled. This problem can be circumvented by using the J–Integral concept. The J–Integral is a global parameter which relates the global loading of a component to the the magnitude of local plastic strain in the vicinity of the crack–tip, thus being capable to characterize the state of load of a crack. The critical value of J, denoted by J_{1c}, characterizes the state of onset of crack–growth.

The most straightforward way of determining J_{1c} is the one according to [6], which is similar to ASTM E813 [7]. These standards are based on the simple relations between energy–consumption and J in the case of a deeply cracked specimen in bending and tension, which were found by Rice et al [8].

In the present investigation CT– specimens of different sizes were used (Fig. 3). The crack extension was measured by the method of partial unloading [6, 7]. The crack–mouth–opening v is measured by a clip gage. An example of v in function of the load F is shown in Fig. 4. From these curve it is possible to calculate the so–called J–resistance–curve (J–R–curve) of the material. The J–R–curves resulting from the CT – tests are shown in Fig. 5. From a J–R–curve one obtains the critical J–Integral J_{1c} as indicated in Fig.5. Its values are given in Table 2. By the equation

$$K_{1c} = \sqrt{[E\, J_{1c}/(1-\upsilon^2)]}, \qquad (1)$$

the fracture toughness can be calculated (E denotes Youngs modulus and υ Poisson's number). The corresponding K_{Ic} are given in Tab.2.

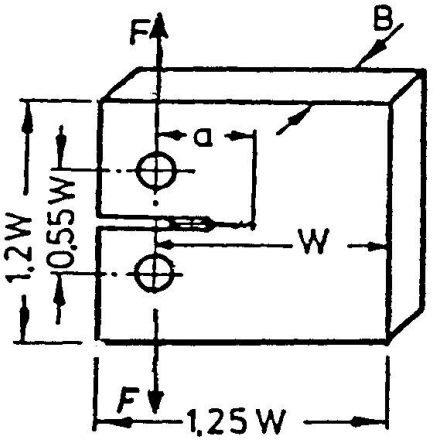

Fig. 3: Geometry of compact tension (CT–) specimen used. For dimensions see Tab. 2.

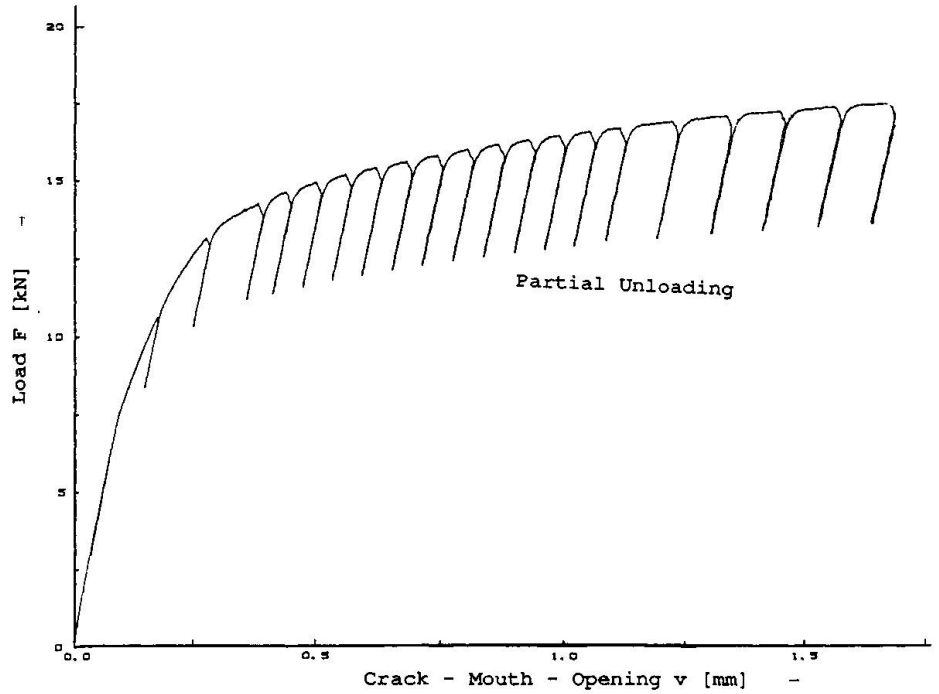

Fig. 4: Example of load vs. crack–mouth opening at load–line as measured on specimen W4

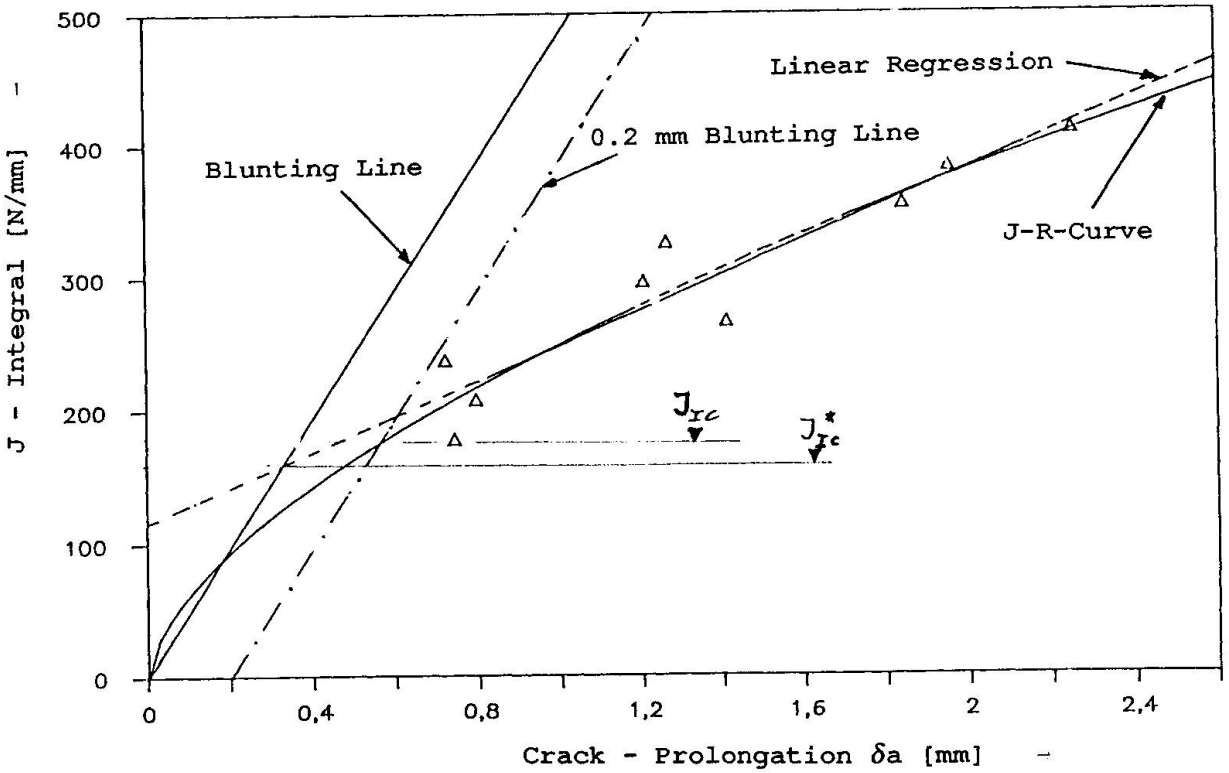

Fig. 5: Example of J–Integral vs. crack–prolongation δa (J–resistance–curve) calculated from load–displacement–curve (Fig. 4) and definition of J_{1c}. For comparision J_{1c} according to ASTM E813–81 (issue 1981 of [7]), denoted by J_{1c}^*, is also shown.

Specimen	W † [mm]	B † [mm]	J_{1c} [N/mm]	K_{1c} [N/mm$^{3/2}$]
W1	25	12	146	5517
W2	25	12	143	5454
W3	50	12	139	5371
W4	50	12	176	6057
† see Fig. 3 for definition				

Tab. 2: Fracture toughness obtained from four tested specimens

3.3. Dynamic fracture toughness

For lower temperature and increased loading rate and different crack–orientation the testing according to paragraph 3.2 becomes much more complicated and costly. Thus these kind of tests were performed on precracked Charpy specimens, loaded by the instrumented Charpy pendulum. The pendulum mass was chosen to be 20 kg, and the impact speed reduced to 1.74 m/s.

A computer program calculated the load–deflection–curve and from this the consumed energy in function of time or deflection for each test. An example is shown in Fig. 6. By means of the following relation, which is based on the results in [8], one obtains the J–Integral from these diagrams:

$$J = K_1^2(a)\,(1 - \upsilon^2)/E + 2\,U_p/t(h-a) \qquad (2)$$

In eq (2) $K_1(a)$ denotes the elastic stress intensity factor for a three–point–bend–specimen with crack–length a (and can be found in the hand–books, e.g. [9]), t the thickness of the specimen, h its width and U_p the plastic part of the consumed energy, i.e

$$U_p = \int_0^{u_p} F\,du_p \qquad (3)$$

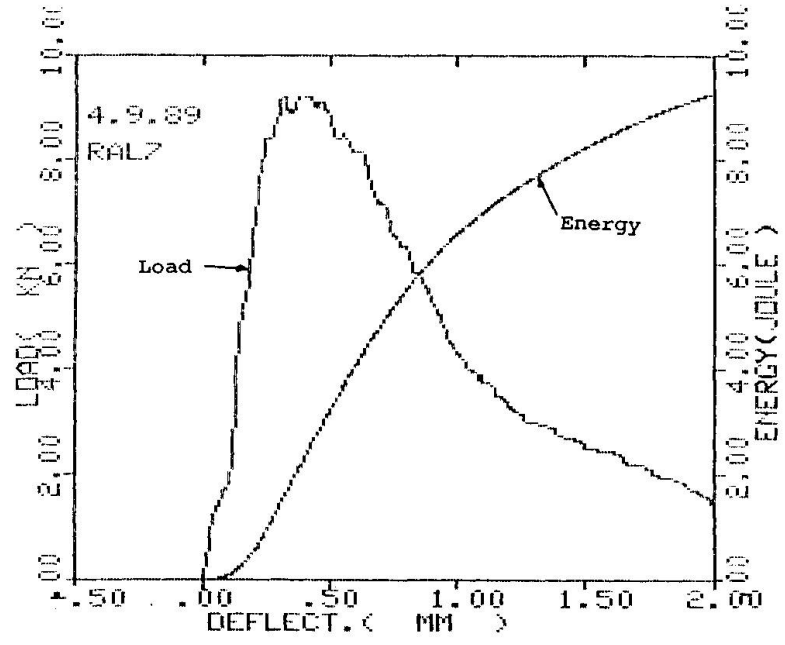

Fig. 6: Example of a load vs. deflection curve and transmitted energy vs. deflection curve of a 3–point–bend impact test with precracked Charpy–specimen. This curve is calculated from the load vs. time curve.

where u_p denotes the plastic part of the beam deflection. If eq.(2) is evaluated at the instant of initiation of crack extension, the resulting J corresponds to a dynamic equivalent of J_{1c} and can be used to calculate the dynamic fracture toughness K_{1d} analogously to K_{1c} by using eq.(1). However, detection of the instant of initial crack–extension on curves like Fig. 5 sometimes is quite difficult and the main source of errors of this procedure. In the present case there are reasons to assume, that crack extension started soon after the maximum load (disregarding the superimposed oscillations) was achieved (a discussion on this topic will be published, [10]). The dynamic fracture toughness obtained by this procedure is shown in Fig. 7.

3.4. Discussion

The J–R–curves (Fig. 5) have two remarkable characteristics mainly: First the initiation toughness, characterized by J_{1c} (resp. K_{1c}), is relatively high, nearly as high as typical values of ordinary structural steel. From the low Charpy impact energy values much lower values were to be expected. Secondly, the gradient of the J–R–curves above J_{1c} is much smaller than in the case of an ordinary structural steel. That means, that the increase of resistance against crack–growth caused by the crack extension is relatively small. This probably explains, why the charpy impact energy is much lower than one would expect from the K_{1c} value.

Whereas the Charpy test exhibited no clear transition behaviour the dynamic fracture toughness measured on precracked Charpy–specimens show a remarkable increase in the temperature range between approximately 0 and 40°C. According to [11] the shift in the transition temperature between static loading and impact loading is about 90°C (for steel with yield–stress of 240 N/mm²). Thus one can conclude, that fracture toughness is at the upper shelf (i.e. approximately 5000 N/mm$^{3/2}$) for all in–service conditions.

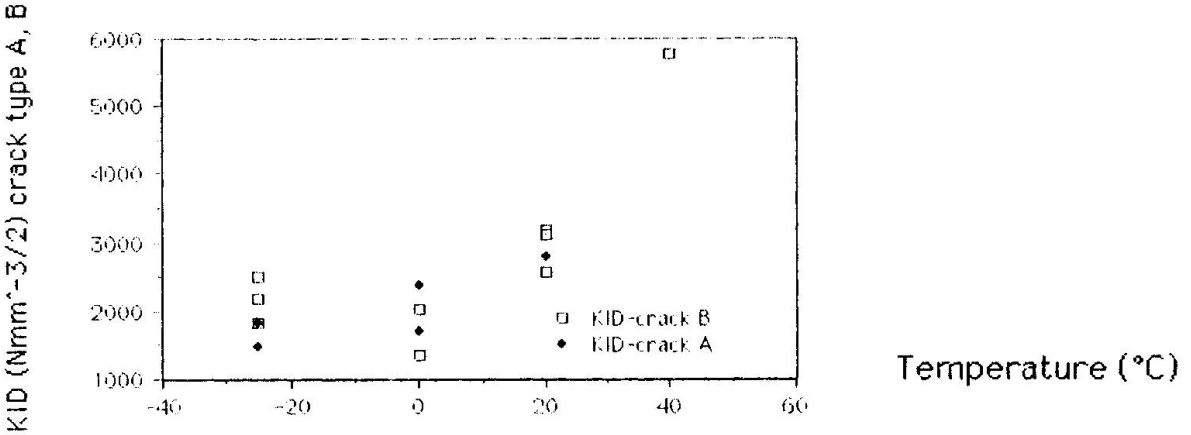

Fig. 7: Dynamic fracture toughness vs. temperature

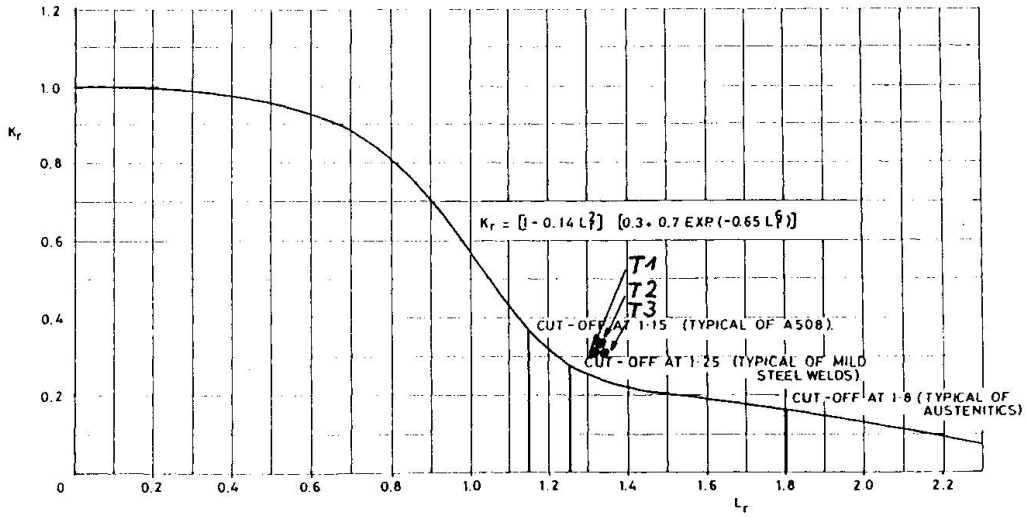

Fig. 8: Failure assessment diagram according to [12]. The points T1, T2 and T3 correspond to fracture tests on precracked component–like specimens

4. FAILURE ASSESSMENT AND CONCLUSIONS

In applying the concept of fracture mechanics to failure assessment of a real structure some difficulties arise: Since the plastic zone ahead of the crack is too large, the theory of linear–elastic fracture mechanics does not apply. On the other hand, performing an analysis of elastic–plastic fracture mechanics is a hard and complex piece of work. For these reasons some relatively simple and easy to–handle methods were developed in recent time. The best known and general accepted methods are the Feddersen–scheme [12], the R6 – Method [13] and the so–called EPRI–"engineering approach" [14]. These methods enable a relatively quick and reliable assessment of the structural safety and integrity on the basis of fracture mechanics.

In the following the application of the R6– method is shortly demonstrated. The central figure of the method is the so–called failure assessment diagram shown in Fig. 8. This diagram reflects the interaction of plastic collapse and crack–instability of a cracked structural component. The horizontal axis contains the quotient of the load L of the considered component divided by the plastic collapse load L_σ the vertical axis the stress intensity factor divided by the fracture toughness. The considered component should be safe, as long as the point corresponding to a given crack–geometry and a given load stays beneath respectively on the left hand side of the failure curve shown in Fig. 8.

If the stresses in a component are not known exactly, it is appropriate to base the failure assessment on conservative assumptions. Given (or assumed, resp.) the stress, the maximum (critical) crack –length can be calculated. In Tab. 3 some critical crack–length corresponding to some typical crack–configurations (see Fig. 9) and conservatively assumed stress–states are given. These results base on the conservative assumtion of K_{1c} to be minimum 4000 N/mm$^{3/2}$.

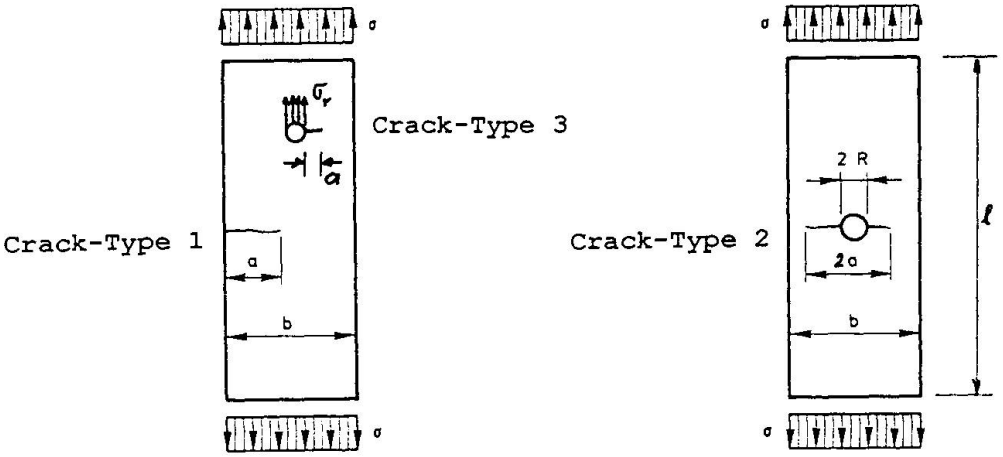

Fig. 9: Definition of crack–types 1, 2 and 3 considered in Tab.3.

In order to verify this failure assessment procedure three tensile tests on precracked component–like specimens were carried out. As test–specimens flat plates of width b = 70 mm, length l = 800 mm and thickness t = 12.5 mm, containing a fatigue crack of a = 18 mm, emanating from a drilled hole of R = 8 mm, were used (see Fig. 9, right hand side). The plates represented a part of a L–shaped profile of the bridge. Since the points corresponding to the maximum measured correspond to unsafe stress–states they are expected to lay slightly outside the safe region of the failure assessment diagram. As shown in Fig. 9 they actually did (Points T1, T2, T3), verifying the R6–method.

The main conclusions from these results are the following: The crack sensitivity of wrought iron is not as high as expected, but comparable with ordinary structural steel. Small cracks which might be missed by visible inspection, e.g. cracks hidden by rivet heads, are hardly able to trigger spontaneous fracture. Structural components which are not weakened by corrosion or visible cracks are supposed to have their original strength.

Crack-type†	loading of component			critical crack size a† [mm]
	axial stress	resid. stress [N/mm²]	rivet stress	
Type 1	240	-	-	22
Type 1	160	90	-	49
Type 2	240	-	-	28
Type 3	240	-	240	10
† see Fig. 9 for definition				

Tab.3: Critical crack sizes for some typical stress-states of a strip- or plate-shaped component made of the investigated wrought iron.

REFERENCES

1. Morf U., Dauerhaftigkeit hochfester Stangen und Drähte mit Zugbeanspruchung, Int. Verb. Brücken– und Hochbau, Lissabon 1989, pp. 199 – 204
2. Varga T., Bewertungssystem der Bruchsicherheit, Schweiz. Bauzeitung 90/91, 1973
3. Brühwiler E., et al, Bewertung der Spontanbruchgefahr angerissener Brückenbauteile aus Schweisseisen, Stahlbau, Vol. 58, 1989, pp 9–16
4. Schweizerische Bundesbahnen, Schweisseiserne Brücken, Teil 2: Materialeigenschaften, Mai 1978
5. Broek D., Elementary engineering fracture mechanics, Martinus Nijhoff Publishers, 1987
6. Deutscher Verband für Materialprüfung (DVM), Ermittlung von Rissinitiierungswerten und Widerstandskurven bei Anwendung des J–Integrals, DVM–Merkblatt 002, Juni 1987
7. ASTM, Standard Test Method for J_{Ic}, A Measure of Fracture Touhness, ASTM E813–87, 1987
8. Rice J.R., et al, Some further results of J–Integral analysis and estimates, ASTM STP 536, 1973, pp. 231–245
9. Tada H., et al., The stress analysis of cracks handbook, Del Research corporation, Hellertown, 1973
10. Schindler H.J., Estimation of J_{1d} by a single impact test, to be published (in Eng. Fract. Mech.)
11. Schwalbe K.H., Bruchmechanik metallischer Werkstoffe, Hanser Verlag, 1980.
12. Central Electricity Generating Board, Assessment of the Integrity of Structures Containing Defects, CEGB R/HR6 – Rev.3 Mai 1986
13. Electric Power Reasearch Institut, An Engineering Approach for Elastic–Plastic Fracture Analysis, EPRI NP–1931, Project 1237–1, July 1981

Leere Seite
Blank page
Page vide

Toughness Requirements for Older Structural Steels

Caractéristiques de résistance d'anciens aciers de construction

Anforderungen an die Zähigkeit älterer Konstruktionsstähle

Kjell ERIKSSON
Lecturer
Lulea University
Sweden

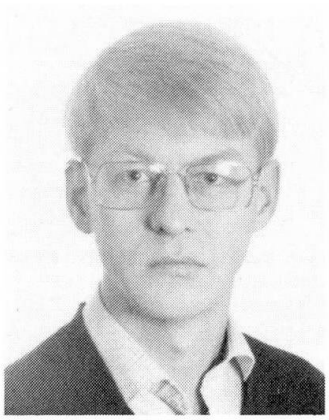

Kjell Eriksson, born 1941, PhD in fracture mechanics 1975, then at Dept. of Welding, Royal Inst. of Technology, Stockholm, Sweden, until 1989. His field is fracture and fatigue of heavy welded steel structures.

SUMMARY

The Charpy-V notch toughnesses of steel from the Swedish railway bridges, 25 – 100 years old, have been found not to satisfy current National Standards requirements. Fracture toughness testing with fullthickness specimens indicate much better effective toughness of a structural part. Also, fatigue crackgrowth rate does not increase with decreasing toughness.

RÉSUMÉ

On a découvert que des résultats d'essais de résilience Charpy-V réalisés sur des aciers provenant d'une dizaine de ponts de chemins-de-fer suédois, datant de 25 à 100 ans, ne correspondent pas aux valeurs courantes données dans les normes nationales. D'autre part, des essais effectués sur des éprouvettes de plus grandes dimensions montrent une résistance effective plus élevée. De plus, la vitesse de propagation des fissures de fatigue n'augmente pas lorsque la résistance diminue.

ZUSAMMENFASSUNG

Zehn verschiedenen, zwischen 25 und 100 Jahre alten schwedischen Eisenbahnbrücken wurden Charpy-Proben entnommen, um die Kerbschlagarbeit zu bestimmen. Dabei zeigt sich, dass die damals verwendeten Stähle die in den aktuellen Normen festgehaltenen Mindestanforderungen nicht zu erfüllen vermögen. Die Ermittlung der effektiven Bauteil-Bruchzähigkeit an Probekörpern grösserer Abmessungen ergibt bei weitem vorteilhaftere Resultate. Weiter stellt man fest, dass die Rissfortschrittsrate mit abnehmender Zähigkeit nicht zunimmt.

1. INTRODUCTION

The one and only national limit on notch ductility came into effect some 30 years ago. In line with the Bonhomme recommendation minimum 27 J Charpy-V notch toughness is required for structural steels in general.

For many years Banverket* has collected Charpy-V notch toughness data of steels from damaged structural elements in railway bridges. The Charpy-V notch toughness of the steels, which are 25-100 years old, is typically 4-7 J at -30°C.

Williams and Ellinger reported in their investigation of the Liberty ship disasters approximately this notch toughness for fracture in combination with severe stress concentrations and welding resid-ual stresses of yield magnitude (or both) in some 30 fracture source plates (1).

The most critical parts for structural integrity of a railway bridge are often plain rolled or riveted beams in which residual stress and stress concentrations are small.

On the other hand severe stress raisers and welding residual stresses are not uncommon due to damage or unskilled repair work, etc.

Despite the very low notch toughness of the damaged steels (and most likely of a much larger number still in service) only partial but unfortunately no catastrophic failures have so far occurred.

These points have risen the question as to the safety and toughness requirements for older railway bridge steels which do not fulfill present toughness requirements.

This paper is based on technical reports on survey investigations carried out on behalf of Banverket. A group of ten steels, of various age and representative of the most brittle, were selected for further investigation. Based on the results a larger testing program has been planned, which adresses the toughness problem of older structural steels.

2. CHARPY-V NOTCH TOUGHNESS

The plate thickness of the investigated steels is typically 10-30 mm. Charpy V notch toughness specimens were machined from the midthickness part of the steel samples. Attempts to register the full notch toughness transition curve always yielded considerable scatter.An example for a typical steel is shown in Fig. 1.

Two series of specimens were tested. The 27 J transition temperature is around +5°C according to the first series and around -25°C according to the second. It is clear that a very large number of specimens is required to avoid an effect of the number of specimens upon the transition temperature.

Even if it were possible to find an unambigous transition temperature the large scatter still implies the question: What constitutes the effective toughness of a structural element?

If the scatter means that the toughness is inhomogeneous on a scale larger than the Charpy specimen, then Charpy notch toughness data is most probably not suitable for toughness requirements of such steels.

*) Swedish National Rail Administration

3. CHEMICAL COMPOSITION

Chemical analysis of the steels is shown in Table 1. All steels are carbon steels. The carbon content is low, usually 0.05-0.10 %, manganese in the range 0.2-0.8 %. The silicon content is typical for rimmed steel, whose inhomogeneous composition is well known. The sulphur and phosphorus contents are not high considering the age of the steels. The total amount of the residual alloying elements (Cr, Ni, Cu) is in the range 0.03-0.15 %. The nitrogen content is 0.004-0.013 %, where N above 0.010 % may cause embrittlement. The Mo and Al contents have also been checked and found to be less than 0.01 and 0.001 % respectively.

Steel	C	Si	Mn	P	S	Cr	Ni	Cu	N
SJ2	0.06	0.01	0.39	0.067	0.035	0.01	0.04	0.08	0.013
SJ4	0.05	0.01	0.46	0.058	0.032	0.01	0.04	0.07	0.012
SJ5	0.15	0.01	0.81	0.060	0.062	0.03	0.05	0.01	0.007
SJ6	0.07	0.01	0.61	0.039	0.028	0.02	0.04	0.01	0.007
SJ7A	0.04	0.01	0.40	0.047	0.037	0.01	0.04	0.05	0.010
SJ7B	0.03	0.01	0.45	0.045	0.037	0.02	0.04	0.04	0.007
SJ8	0.10	0.01	0.63	0.071	0.071	0.02	0.04	0.01	0.011
SJ9	0.15	0.02	0.27	0.068	0.020	0.02	0.01	0.05	0.004
SJ10	0.19	0.02	0.22	0.030	0.010	0.01	0.01	0.01	0.011

Table 1 Chemical analysis wt%

4. FRACTURE TOUGHNESS

To obtain an alternative estimate of the effective toughness of a structural member, fracture toughness testing was carried out. Full thickness Compact specimens were cut from plates or beam flanges and subsequently fatigue precracked at room temperature. The crack plane is always perpendicular to the rolling direction of the parent steel. Specimen data are given in Table II.

Steel	Form	Year	W(mm)	B(mm)
SJ2	I-beam	1915	160	27
SJ4	-"-	1920	128	20
SJ5	-"-	1940	240	27
SJ6	-"-	1940	160	15
SJ7A	plate	1922	128	14
SJ7B	-"-	1922	128	14
SJ8	I-beam	1940	160	19
SJ10	L-profile	1900	60	20
SJ11	I-beam	1919	100	26

Table II Fracture toughness specimen data

Fracture toughness testing was carried out according to ASTM Standard E813-87 when applicable (2). The test temperature was -30°C. During a test the load versus load point displacement curve was registered. Although the registered curves in general were non-linear, no evidence of stable crck growth was found. For each curve J_c was evaluated according to Merkle and Corten (3).

Uniaxial tensile testing data (at room temperature), Charpy-V notch toughness and fracture toughness are given in Table III.

Steel	R_{eL} (MPa)	R_m (MPa)	A_5 %	Charpy-V notch toughness 1) C_v(J)	Fracture toughness J_c(kN/m)
SJ2	246	386	32	4.8*)	22
SJ4	230	365	38	5.3*)	145
SJ5	239	449	34	6.9	22
SJ6	233	380	39	6.6	122
SJ7A	253	388	25	5.9	>400
SJ7B	258	394	29	4.1	177
SJ8	239	439	31	5.9	21
SJ9	330	486	23	5.3	28
SJ10	258	440	25	5.3	15
SJ11	263	385	34	3.4	8

*) Test temperature 0°C
1) Mean of three measurements

Table III Charpy notch toughness and fracture toughness

5. FATIGUE CRACK GROWTH

The most brittle steel, SJ11, of the ten investigated was selected for fatigue testing. Low cycle fatigue crack growth in Compact specimen was recorded at room temperature.da/dN versus ΔK data were analyzed according to Paris´law and the fatigue threshold was determined. The results are given in Table IV.

Test no	ΔK_{th} (MN/m$^{3/2}$)	C	n
1	8.8	$3.76\ 10^{-12}$	3.2
2	6.5	$2.60\ 10^{-12}$	3.3
3	5.5	$3.20\ 10^{-12}$	3.2

C and n are the constants in Paris´law for da/dN in m/cycle.

Table IV Low cycle fatigue crack growth

6. DISCUSSION

The relationship between fracture toughness (J_c) and notch toughness (C_v) for the steels in this investigation is compared with others in Fig. 2.

All steels are tougher according to J_c than to C_v compared to the corresponding relationship for homogeneous steels (6). The steels in this investigation might be divided into two groups depending upon the relation between J_c and C_v.

In the first group the steels are twice to four times tougher according to J_c and to C_v. The steels in this group are brittle both according to Charpy-V notch toughness and to fracture toughness.

In the second group the steels are more than ten times tougher according to J_c and C_v. The steels are in fact brittle according to C_v and ductile according to J_c.

We assume this is because the toughness of these steels is (very) inhomogeneous, particularly in the second group. In rolled steel the toughness varies across the

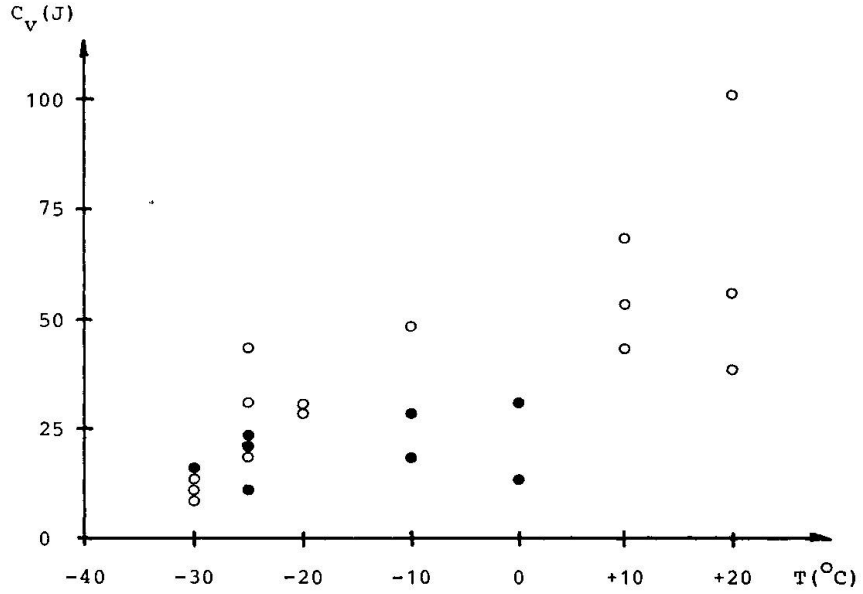

Fig 1. Charpy-V notch toughness for two specimen series of a given material. o Ser no 1. ● Ser no 2.

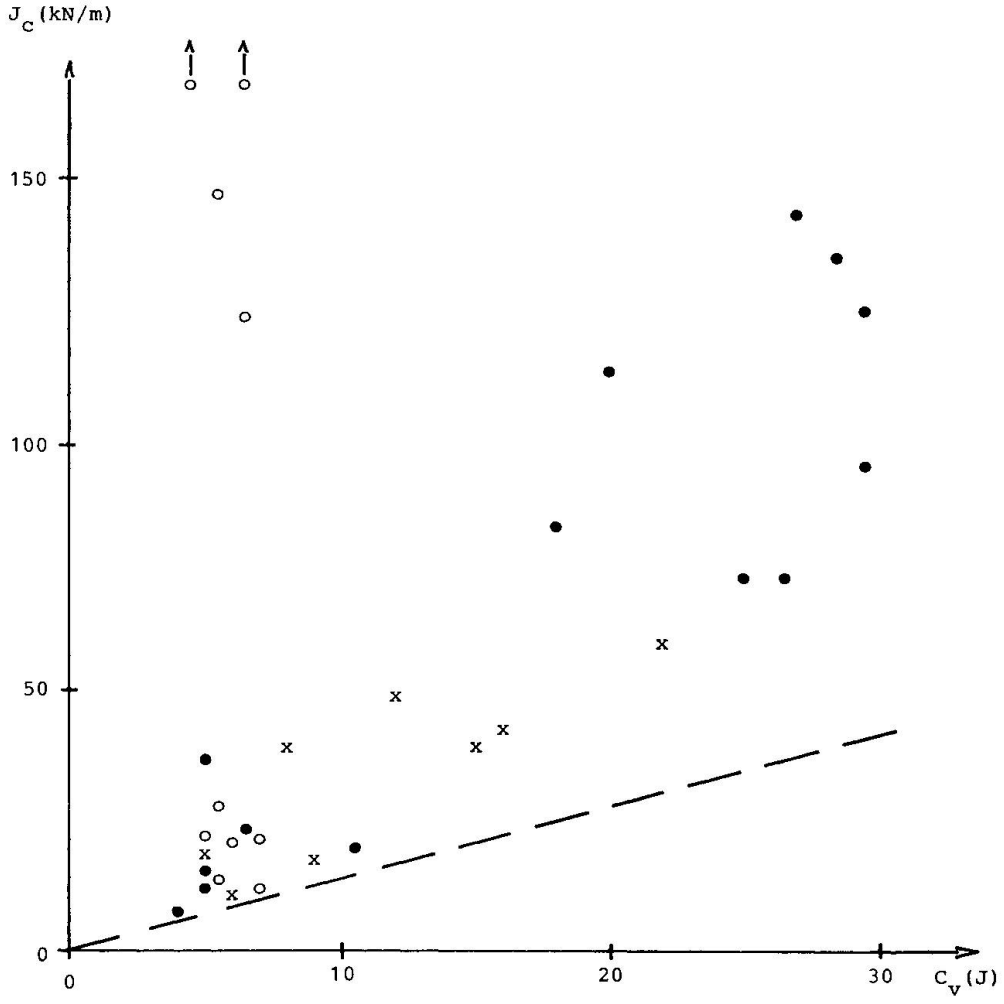

Fig 2. Fracture toughness J_C and Charpy-V notch toughness C_V. o This investigation, x Ref (4), ● Ref (5). - - - Ref (6).

thickness and is higher near the surface than in the middle. The thickness distribution may also vary from point to point in the rolling plane.

In a full thickness fracture toughness specimen the entire toughness distribution in the thickness direction is represented along the crack front. Thus J_c obtained with full thickness specimens represents the effective toughness of a plate or beam flange, etc.

A Charpy specimen on the other hand has always fixed dimensions.In our investigations the Charpy specimens were always machined on all sides and taken from the mid-thickness. A Charpy specimen therefore only represents a small part of, most linkely, low toughness material.

This effect would also explain the fact that no catastrophic failures have occured in spite of Charpy notch toughness no better than that associated with the Library ship disasters. The question as to the real safety of the steels has however not yet found an answer.

To ensure plain strain conditions at a crack tip in elastic-plastic fracture toughness testing the condition $t > \alpha J_c \sigma_y$ has been proposed (7). t is specimen thickness, α a numerical constant in the range 25-50 and σ_y is flow stress.

Now to obtain a minimum toughness requirement we simply turn this condition around and require that

$$J_c > \beta\sigma_y t$$

where β is a dimensionless constant for the time beeing put to 0.02. This toughness is just enough to prevent plain strain conditions at a crack tip. The conditions means that if a structure fails, it fails in a ductile manner, whatever the size of a crack.

It is interesting to note that this condition is fulfilled by the steels in our second group but not by those in the first.

Although the steel selected for fatigue testing is the most brittle, its crack growth data is typical for structural steel. This means that fatigue cracks do not grow faster in a low-toughness structural steel.

The fatigue threshold is also typical but there is some scatter.

The crack growth data is a mean value over several mm of growth and thus local variations, if any, are levelled out. The threshold, on the other hand, involves propagation over a very small distance and thus local variations may strongly affect its value. The treshold scsatter is thus a further indication of an inhomogeneous material.

A low fatigue threshold and a small critical crack size means of course reduced residual life in spite of typical crack growth data.

7. FUTURE WORK

The structural elements from which damaged parts have been collected are mostly plain rolled or riveted beams of various cross-sections but with heights not exceeding 500 mm. If there is an effect of size upon fracture behaviour then data for large structures (ships) may not be applicable to smaller structures (beams). It is doubtful whether it is possible to check this by using Charpy even for an ideally homogeneous material.

In the fracture thoughness testing program some amount of plastic deformation, although in some cases very samll, always preceeded fracture. If a ductility criterion is to be based upon J_c then the amount of plastic deformation predeeding fracture must be of such an extent that an effect of size upon J_c may be expected.

To determine the minimum toughness requirement for a (small) specimen that corresponds to a given safety for a (large) structural member full scale bend testing of HEB 400 beams has been organized. Experimental validation of the condition (a) is part of this work. The results will be reported in a forthcoming paper.

REFERENCES

1. WILLIAMS M.L.& ELLINGER G.A., Investigations of Structural Failures of Welded Ships. The Welding Journal 32(10), Research Supplement, 1953, pp 498-527.
2. ASTM Standard E813-87, Standard Test for J_{Ic}, a Measure of Fracuture Toughness, Annual Book of ASTM Standards. ASTM, Philadelphia, 1987.
3. MERKLE J.G. & CORTEN H.T., a J-Integral Analysis for the Compact Specimen. Journal of Pressure Vessel Technology, Nov.1974, pp 286-292.
4. MARANDET B & SANZ G, Étude par la mécanique de la rupture de la ténacité d´aciers a résistance moyenne fournis en forte épaisseur. Révue de Métallurgié, Avril 1976, pp 359-383.
5. SSAB Technical report SF 154/83 on correlation between K_{Ic} and C_v. In Swedish.
6. SAILORS R.H. & CORTEN H.T., Relationship Between Material Fracture Toughness Using Fracture Mechanics and Transition Temperature Tests. ASTM STP 514, ASTM, Philadelphia, 1973, pp 164-191.
7 MCMEEKING R.M. & PARKS D.M., On Criteria for J-Dominance of Crack-Tip Fields in Large-Scale Yielding. ASTM STP 668, ASTM, Philadelphia, 1979, pp 175-194.

Leere Seite
Blank page
Page vide

Crack Growth Tests to Assess the Remaining Fatigue Life of Old Steel Bridges

Essais de propagation de fissures pour estimer la durée de vie restante d'anciens ponts en acier

Risswachstums-Versuche zur Schätzung der Restlebensdauer alter Stahlbrücken

Klaus BRANDES
Dr.-Ing.
BAM
West-Berlin

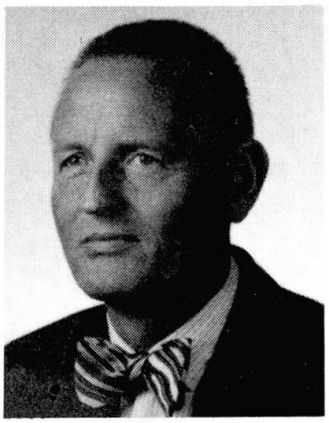

Klaus Brandes received his graduate as well as his doctorate at the Technical University of Berlin. After working for some years in the field of steel structures, he went to the Federal Institute of Materials Research and Testing (BAM) in 1968 where he is concerned with various fields of structural engineering.

SUMMARY

While evaluating the remaining fatigue life of old steel bridges, a complementary test has been employed a crack growth test for standardized specimens. The findings of these tests assist the evaluation in two ways. Firstly, an estimate of fatigue strength can be made, and, secondly, the propagation of existing and postulated cracks can be predicted.

RÉSUMÉ

Pour l'évaluation de la durée de vie restante d'anciens ponts en acier, un outil complémentaire a été utilisé – des essais de propagation de fissures sur des éprouvettes standardisées. Les résultats d'essais apportent deux améliorations distinctes. D'une part, une estimation de la résistance à la fatigue peut être faite, et, d'autre part, la propagation de fissures existantes ou postulées peut être prédite.

ZUSAMMENFASSUNG

In das Verfahren zur Ermittlung der Restnutzungsdauer alter Stahlbrücken ist ein zusätzliches Hilfsmittel einbezogen worden – Rissfortschrittsversuche an Standard-Proben. Aus den Ergebnissen dieser Versuche folgen zwei Verbesserungen des Verfahrens. Zum einen kann die Ermüdungsfestigkeit des Materials geschätzt werden, und zum andern kann das Anwachsen vorhandener oder postulierter Risse vorausgesagt werden.

1. INTRODUCTION

Many old riveted steel bridges in different countries approach now their hundredth birthday - or even more - and very often, there is no reason to put them out of service. The replacement of all these bridges far exceed the available financial resources. However, even if the funds existed, in several cases replacement would be the least acceptable option because many of the bridges are of historical importance [1] [2] [3].

During the last years, repeatedly the question emerged whether or not an old bridge should be preserved for the future and should remain under (full) traffic load for some more decades.

Applying the procedure of rating old bridges as specified e. g. by Hirt [6], we decided to add a supplementary element qualified for characterizing the fatigue behaviour of highly stressed structural elements: Crack growth tests as being well known from other fields of engineering.

As we found by performing the incorporation of this additional tool, it offers more than only confirmation of the fatigue strength characteristics of structural elements.

Figure 1. Steel bridge of the Berlin Metropolitan, built in 1898, replaced 1988

2. MOTIVATION OF THE INVESTIGATION

During some years, we have been concerned with the rating of old steel bridges, the most of them in Berlin, however some of them in West Germany. It is not even a simple task to produce evidence that an "overdue" bridge may be kept in service. After having executed all the steps of the procedure of evaluating the remaining fatigue life of highly stressed structural members, we tried to identify the fatigue behaviour of the material produced more than hundred years ago. Presuming that the growing of cracks under repeated loading will be the governing physical effect of fatigue [7], we performed crack growth tests on samples of the structural members in question.
However, as a result, it was not only possible to answer the question of similarity of the steel of the turn of the century and that of today: The direct application of the crack propagation concept to structural members had the

consequence of looking to the structural details having in mind to find where the first crack could occur.

In this context, it is not only important to look at the structural details for rating a certain bridge for its further use. There is the other task to approve the procedure of rating by fatigue-loading old bridges up to the point of having large cracks. This task can only be done after putting bridges out of service and simulate traffic load, preferably in the laboratory. This kind of loading of these bridges (constant-amplitude loading, variable-amplitude loading) should be discussed to get as much information from these tests as possible (see e. g. [9]).

In the following, three main topics shall be presented and discussed.
- Crack growth tests and its results
- Application of fracture mechanics approach to bridge's structural members
- Measured stresses (strains) and the treatment of small stress cycles.

Figure 2. Truss girder bridge of the Berlin Underground, built in 1902, replaced in 1989

3. CRACK GROWTH TESTS; RESULTS

Up to now, crack growth tests have been included in the investigation of three bridges in our institute [5] [8]. The first one, a road bridge, was built in 1952 with unidentified material from the thirties. The other ones, two parallel bridges of the Berlin Metropolitan, fig. 1, were erected in 1898. The latter ones are now replaced because of widening of the streets they crossed. In all cases, we measured strains under traffic. The two bridges of the Berlin Metropolitan will be used as models of natural size to evaluate their fatigue life after hundred years of loading, maintance and corrosion.
Today, we perform cyclic loading tests on parts of the Berlin Underground Bridge shown in fig. 2, which was built in 1902.

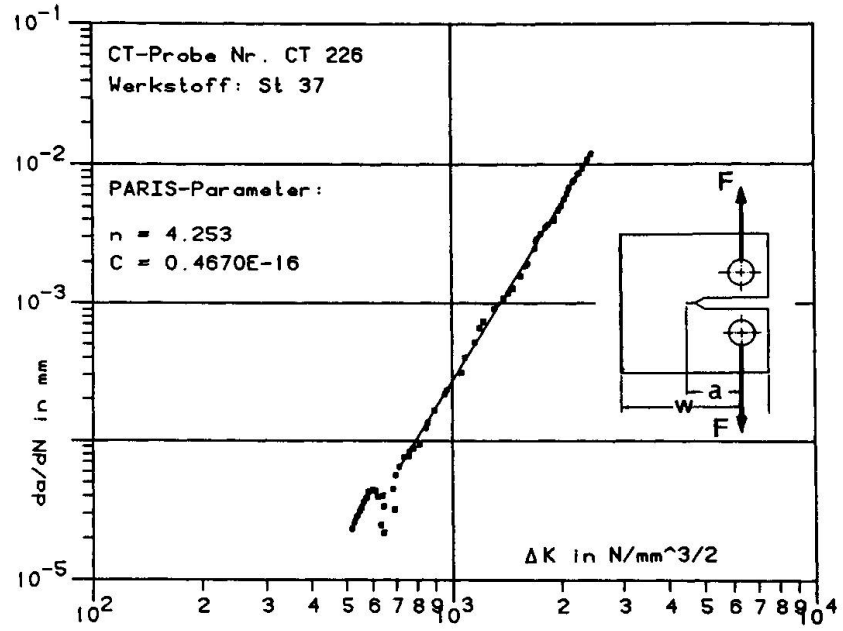

Figure 3. Result of one of the crack growth tests (ASTM E 647-83) with regression line regarding the Paris equation (1)

The crack growth tests which supplemented the set of standard technological tests (strength, chemical analysis) were performed according to ASTM E 647-83 [10]. The specimens were 12.5 mm thick. The initial value of the cyclic stress intensity factor ΔK reached 300 N/mm$^{3/2}$ to 500 N/mm$^{3/2}$.

The results of the tests, given in terms of the Paris-equation, fig. 3,

$$da/dN = C\,\Delta K^{n} \qquad (1)$$

a crack length
N number of loading cycles
ΔK cyclic stress intensity factor
C;n material parameters of crack groth

have proven that there is no significant difference between mild steel produced at the turn of the centuries and today.
The value of n tends to a little bit higher values than presented in textbooks for present-day steel

$$n = 2.83 \ldots 4.75.$$

However, relatively large values of n correspond to very small values of C,

$$C \approx 10^{17} \quad \text{for } n > 4.3.$$

Thus, high values of crack growth for moderate values of ΔK appear for small values of n and large values of C, e. g. n = 3 and C = 10^{-13}.
From our crack growth tests on specimens of steel produced about 100 years ago - up to now a rather limited number of tests - we can deduce that this steel behaves like present-day steel concerning fatigue.
For the future investigations we intend to include the evaluation of the threshold-value of ΔK for crack growth that has a certain relationship to the cut-off limits of the fatigue strength curves.

In this connection, it should be mentioned that the characteristic values of strength (yield, stress, tensile strength) of the material in question reach about 230 N/mm² and 360 N/mm², respectively; the total elongation at fracture reaches about A_5 = 30 %.

4. APPLICATION OF FRACTURE MECHANICS TO STRUCTURAL MEMBERS

The application of fracture mechanics in the evaluation of remaining fatigue life implies the modelling of cracks in structural members, which can presumably appear, fig 4. The propagation of cracks then is only governed by the stress intensity at the crack's tip as expressed by the Paris equation. On this basis, it is possible to predict how far a certain crack can grow within the period of time between two inspections.

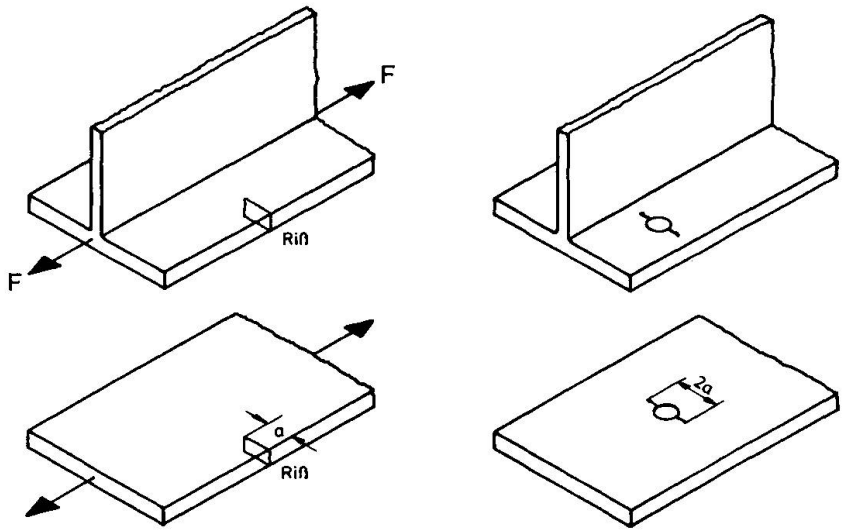

Figure 4. Crack patterns in riveted members for evaluating stress intensity factors and crack growth

It is an advantage of fracture mechanics to enable this kind of prediction and to lead to a deeper insight into the problem of survival of structural members under cyclic loading than only the application of fatigue strength curves can generate.

5. HIGH-CYCLE FATIGUE STRENGTH AND FATIGUE LIMITS

The long-life fatigue behaviour of welded structures has been subject of discussion and research quite recently [9]. However, the same problems occur for old riveted structures, too. Looking at the results of measurements at some bridges, we found that only very few of the stress cycles exceed the cut-off limits as given e. g. in the ECCS Recommendations [11], fig. 5.
Because of the fact that the allowable stresses about 100 years ago reached about 90 N/mm² or even 120 N/mm², the stresses in structural members of bridges of the Metropolitan or Underground in Berlin reach under traffic only 30 N/mm² or even 50 N/mm². Maybe, that in the past, in the course of an eventful history, overloadings could have taken place. This uncertainty of the loading in the past makes it complicated to judge the fatigue damage that bridges could have experienced during service life.
However, looking at what happens during crack growth tests, it seems that only a few cycles of high loading do not influence the crack growth significantly. This does not necessarily hold for loadings in the threshold stress range as expressed in [9] by the sentence: Stress ranges below the constant amplitude fatigue limit (CAFL) influence the fatigue life if there is at least one cycle in the variable-amplitude spectrum above the CAFL.

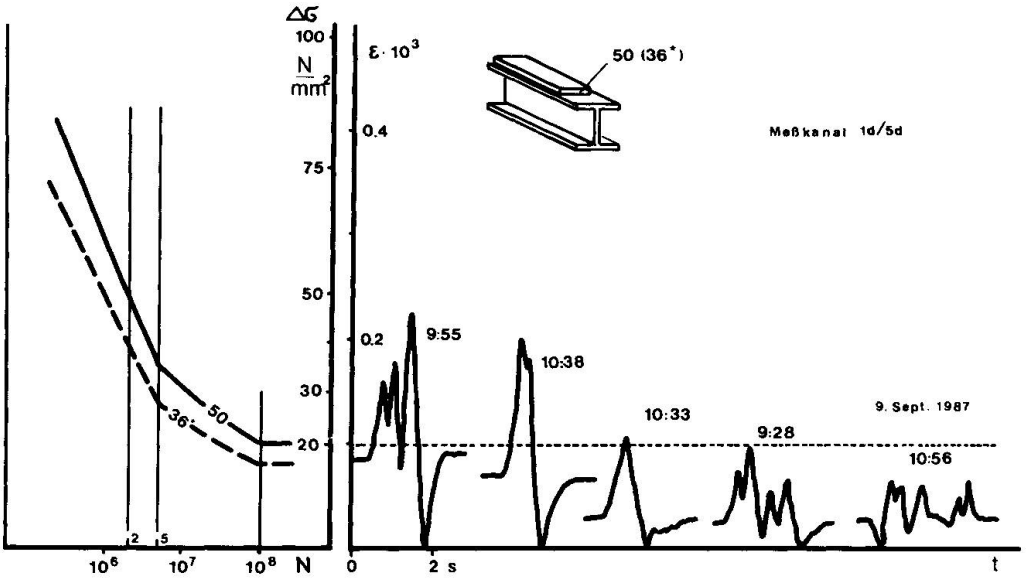

Figure 5. Measured strains/stresses during about 3 hours of observation at one measuring point.
The curves on the right hand side represent the largest measured cycles (indicated: time of vehicle passing) [5] which are compared with the cut-off limits of the ECCS-fatigue strength curve 50 (36*) [11]

6. EXPERIMENTS WITH OLD BRIDGES

In the Federal Institute for Materials Research and Testing (BAM), we started with experimental investigations the subject of which are complete small-span bridges or parts of larger ones. In some case, we could measure strains under traffic flow before they were replaced. There are many questions that should be answered. However, in a first step, we are going to apply constant-amplitude loading that generates in the structural members stresses in the range we measured before.
The most of the loadings will be in the range near the CAFL. For the future investigations, we are going to discuss in which stress range we should perform the tests.
We hope that we can contribute to improve the answers on the question for how much longer a certain bridge will carry the loading within certain limits of safety margins.

REFERENCES

[1] KIM, J.B., BRUNGRABER, R.J. and KUN, R.H., Recycling Bridges. Civil Engineering, Nov. 1988, pp. 58/59

[2] GREENE, P., Bridge Restored for Earlier Form. Eng. News Records, 217 (1986, p. 32 (see also: OHLEMUTZ, A., Roebling-Brücke von 1847 wird restauriert. Stahlbau 57 (1988), pp. 121/122)

[3] BUCHMANN, F.-U., Die ersten eisernen Viadukte für die Eisenbahn in Frankreich (1864-1969). Stahlbau 59 (1988), pp. 193-197

[4] OEHME, P., Damage Analysis of Steel Structures (in German). IABSE Periodica 4/1989 - IABSE Proceedings P-139/89, pp. 121-140

[5] BRANDES, K., Investigations of Crack Growth on a Steel Bridge (in German). Congress Report, 13th Congress IABSE, Helsinki, 1988, pp. 361-366

[6] HIRT, M.A., Remaining Fatigue Life of Bridges. Proceedings, IABSE-Symposium: Maintenance, Repair and Rehabilitation of Bridges, Washington, D.C. 1982

[7] KOSTEAS, D., Grundlagen für Betriebsfestigkeits-Nachweise. In: Stahlbau-Handbuch, Stahlbau-Verlag, Köln 1982, Seiten 585-618

[8] BRANDES, K., Remaining Fatigue Life of Old Steel Bridges. IABSE-Symposium: Durability of Structures, Lisbon, Sept. 6-8, 1989, pp. 365-370

[9] SMITH, I.F.C., CASTIGLIONI, C.A. and KEATING, P.B., Analysis of Fatigue Recommendations Considering New Data. IABSE Periodica 3/1989, IABSE Proceedings P-137/89, pp. 97-109

[10] ASTM E 647-83. Standard test method for constant loading amplitude crack growth rates above 10^{-8} m/cycle.

[11] ECCS-Technical Commission 6 - Fatigue -: Empfehlungen für die Bemessung und Konstruktion von ermüdungsbeanspruchten Stahlbauten. SZS-Publikation 43, 1987

Leere Seite
Blank page
Page vide

Update on Fatigue Issues at Canadian National Railways

Conclusions récentes des chemins de fer nationaux canadiens dans le domaine de la fatigue

Neuste Erkenntnisse des «Canadian National Railways» zur Ermüdung

Robert A.P. SWEENEY
Director Structures
Canadian National Railways
Montreal, PQ, Canada

Robert Sweeney is the Chairman of A.R.E.A. Sub-Committees on Rating and Fatigue Design Requirements, as well as the Chairman of the AAR-NSF Committee on Railroad bridge testing.

SUMMARY
The paper deals with issues of bridge testing, rivet replacement with high strength bolts, accoustic emission testing and the validity of current fatigue strength curves for riveted connections and corroded members. A brief discussion of Safe Life Techniques, used to predict bridge component lives, is included together with system costs on the effect of fatigue damage.

RÉSUMÉ
Cet article traite des sujets concernant des essais sur des ponts, le remplacement des rivets par des boulons à haute résistance, des méthodes de contrôle accoustiques, et la validité des courbes caractéristiques de la résistance à la fatigue des assemblages rivetés et des éléments corrodés. Il donne également une brève discussion des méthodes de calcul de la durée de vie, utilisées pour évaluer la durée de vie des éléments de ponts, ainsi que de l'effet du dommage en fatigue sur les coûts.

ZUSAMMENFASSUNG
In diesem Artikel wird über Erkenntnisse im Zusammenhang mit Brückenversuchen, Ersatz von Nieten durch hochfeste Bolzen und akkustische Prüfmethoden berichtet. Zudem wird untersucht, inwieweit die üblichen Ermüdungsfestigkeitskurven für Nietverbindungen und korrodierte Bauteile Gültigkeit haben. Ein kurzer Abriss über Techniken zur Voraussage der sicheren Lebensdauer von Brückenelementen ist ebenso enthalten wie einige Anmerkungen zum Einfluss von Ermüdungsschäden auf die Systemkosten.

The railway industry in North America is facing a further 20% increase in Axle loadings. In August of 1989, CN received its first regular Double Stack trains with 35.7 tonnes (78,750 lbs) Axle Weights. The previous limit of 30 tonnes (65,650 lbs) had been in effect from the early 1960's.

In view of the fact that the major bridge building era for CN occurred before 1915 most of our major steel bridges are over 75 years old.

These new loadings put at risk 6 to 7 times the number of connections.

At CN we have been using Safe Life techniques to assure safe railway operation Vis a Vis major potential fatigue distress. The principle is that it is better to replace number of bridge components a few years too soon rather than have one bridge replaced too late.

Our long term objective is to reduce the uncertainty and only replace the critical components as they became critical. This is perhaps a dream but still a worth while objective.

Using the existing AREA rating manual (1) and evaluating the remaining useful lives of our main line bridges based on the 2.3% probability curves used in that document, but with actual historical trains and estimated future traffic, led to an indicated increase of bridge replacements from roughly $3.5m U.S. to $23m U.S. annually over the next 25 years.

The procedure is relatively straight forward (Fig. 1). A root-mean cube stress range and relevant cycles are estimated using the rain flow method. This is plotted against the code detail limit on an S-N diagram for traffic to date and various future traffic projections. The remaining detail life is thus estimated.

If 0.1% of the stress ranges have exceeded the constant amplitude fatigue limit, the limit is assumed not to exist and the S-N line is extended downward at the same slope (2).

Given the remaining detail life it is straight-forward to estimate costs for repairs, retrofits, strengthening or replacement as appropriate.

Since severe fatigue distress has already been observed and calibrated with the methods used this leads to the realization of a major cash flow problem.

The bridge section immediately began searching for ways to reduce the expenditure and obtain more reliable ways to manage the situation. Anything that can attack the 2.3% probability criterion and give more certainty would be of value.

The first action taken was to increase the number of spans tested from an average of 2 to 25 per annum. A mobile testing outfit was purchased and developed containing all the

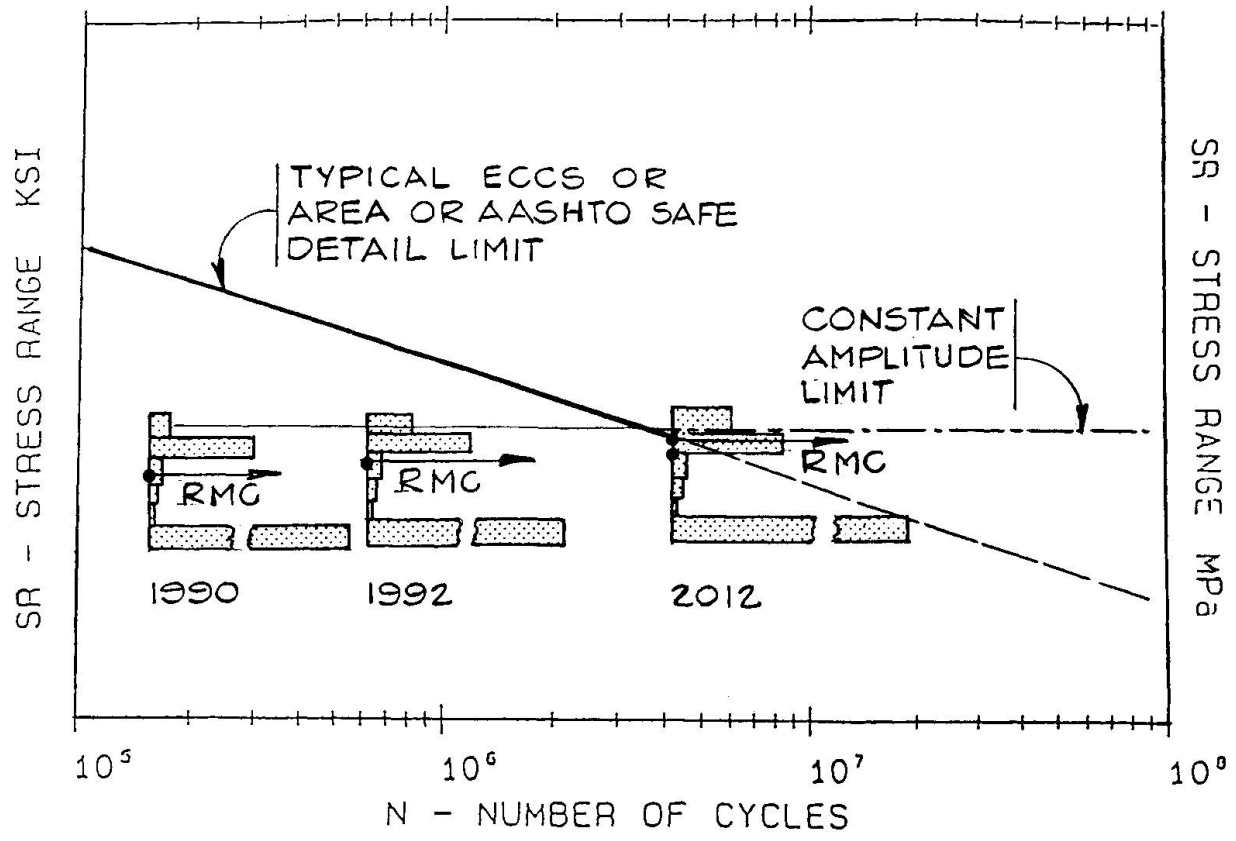

Fig. 1

necessary computers, fibre optic cables, etc. to record up to 24 locations at 1,000 Hz, and to leave a recording device for up to 6 months un-monitored to obtain longer term histograms.

The writer as chairman of the American Railway Association - National Science Foundation Committee on Railway Bridge Testing has seen to a similar program in the United States. To date a Burlington Northern deck plate girder bridge in Illinois has been tested. A bridge on the Norfolk-Southern railroad in Virginia which carries one way fully loaded unit coal trains is under test at the present time (March 1990).

The resultant lower than mathematically modelled stress ranges measured, and subsequently mathematically justified, in all but two CN cases led to a postponement of $7m worth of bridge replacement on the first 25 CN structures measured under real trains.

The next step for CN was to develop in conjunction with Monac, a firm developing a technique put forward by Professor N. Bassim of the University of Winnipeg, an artificial intelligence routine to use accoustic emissions to predict the status of cracking in relation to its position on the "Paris" law curve. The technique was verified at the ATLSS lab at Lehigh University on a series of beams undergoing high cycle fatigue testing. Field testing was done on the Lehigh Canal bridge, and two CNR bridges.

The result is a value for the change in stress intensity factor, K together with the crack growth rate, da/dn. At 22MPa$\sqrt{m}$ (20ksi $\sqrt{in}$) we start to be concerned and would cease operating at 44MPa$\sqrt{m}$ (40ksi$\sqrt{in}$) on our older steels.

This technique was applied to 11 bridges in 1989, and led to the postponement of 7 jobs, the change from replace to retrofit and strengthening on 2 jobs, and the immediate replacement as planned of two bridges.

Presumably working with a 2.3% probability of failure one would expect less than 1 bridge out of 11 in need of replacement. We found two. Some of the critical components will be examined after the bridges are dismantled to gain further confidence in the technique.

Monac testing will have to be repeated to ensure that crack growth rates are not accelerating as traffic patterns change.

Existing North American fatigue criteria on rivets indicates problems above MPa (7 ksi) stress range if 0.1% of all loads exceed the constant amplitude fatigue limit value of 48 MPa (7ksi) for category D (ECCS71) (2).

The slope of the SN curve for welded, riveted and bolted details is - 3 (log scale). Since many girders spans have 100 or more rivets making the cover plate to flange connections, and since the critical crack size is just slightly larger than the rivet head diameter making detection difficult, an economical way of removing rivets, and replacing these with higher fatigue category High Strength bolts is required without damaging the existing steel. Removing 2 or 3 rivets works fine, but removing 100 or so rivets with a 16kg (35 lbs) tool is bound to lead to some nicks or gouges in the flange creating a worse detail.

CN has commissioned a pilot study at Lehigh University's ATLSS Center to investigate the feasibility of a better tool.

Techniques evaluated to date include:

1. Water Jet cutting at pressure rates near 410 PMa (60 ksi)
2. Laser cutting
3. Nitrogen freezing and subsequent impact
4. Grinding and twisting
5. Better pneumatic tools
6. Refined chisels
7. Efforts to reduce tool weight and resultant operator fatigue as well as set-up time
8. Head removal tools
9. Core drilling
10. Hydraulic removal tools

After preliminary study, techniques 3,5,6 and 7 are being pursued further.

I would like to draw your attention to the current recommended North American criteria for rivet fatigue evaluation (Fig. II). There is little relevant test data on real structures in the shaded segment of the diagram (3, Fig. 32) (5). Furthermore it would appear that a different slope somewhere between -4 and -5 also fits the data quite well (heavy line).

If the heavy line were to be valid a considerable number of structures would not be at risk for quite some time. The example in figure II indicates over twice the life for the same probability of failure. The two step ECCS curve addresses this somewhat below 48MPa (7ksi), but does not deal with the problem in the 48MPa (7ksi) to 83MPa (12ksi) stress range. My gut feeling is that a slope appropriate to welded and plain material may not be appropriate for mechanical fasteners.

North American experts suggest that more variable-amplitude testing in the shaded segment is necessary to confirm this. This would be very desirable.

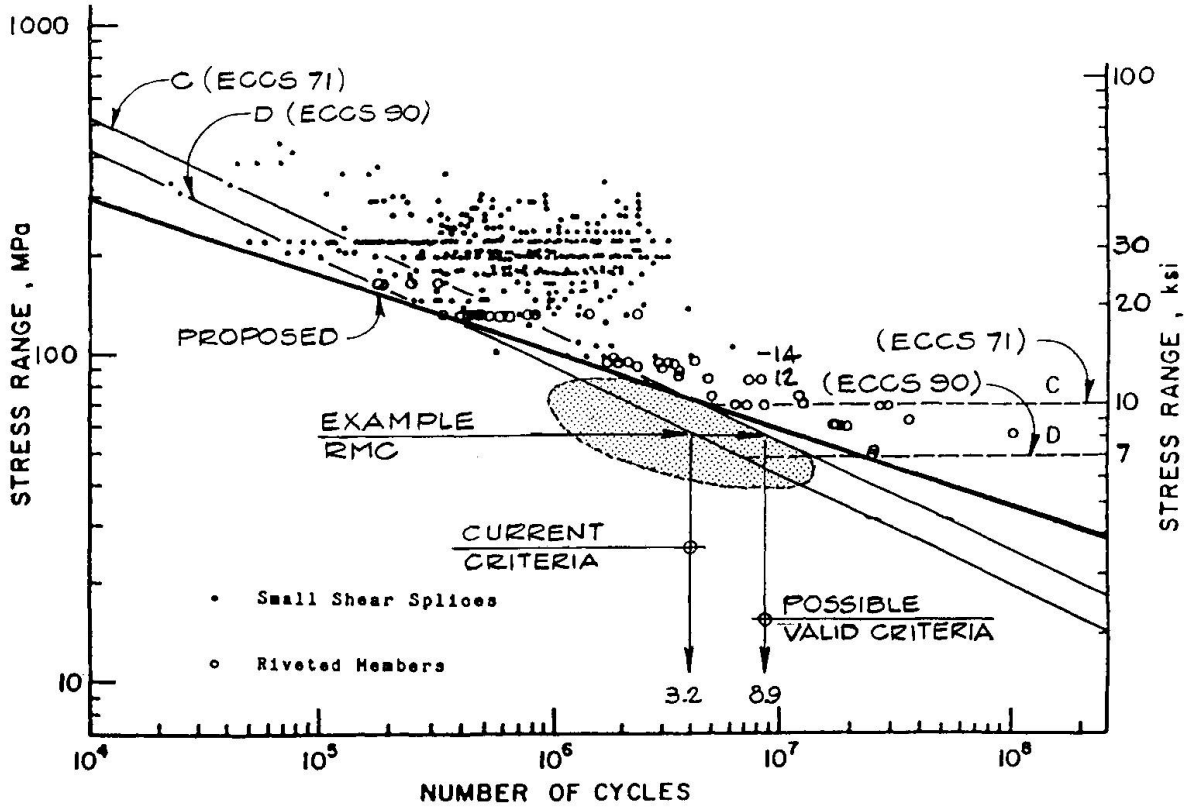

Comparison of fatigue resistance of full-size members with small shear splices. (3, FIG.32)

Fig. 2

Recent tests on badly corroded girders indicate that corrosion cell activity accelerates in poorly corroded beams. From a fatigue point of view current thinking suggests that one must assume a category E or E' detail depending on component thickness at any location where the original section has been reduced by more than 50% (2). Work by Albrecht (4) on sections pitting with up to 21% section loss on weathering steel indicates a reduction from category "A" (ECCS 160) to category "C" (ECCS 90) and he recommends introduction of a pitting factor.

On our railway the first criteria adds $300m to our 25 year bridge replacement bill if it is applied blindly. Clearly this will not be done.

The Albrecht criteria has not been applied since rivets are already the controlling detail in older structures.

Much more research is required to develop more rational criteria in this area, particularly for very badly corroded components.

In summary, it is felt that more testing will lead to:

1. a different slope on the S-N diagram for riveted connections, leading to predictions of longer component lives, and

2. a more rational criteria for badly corroded bridge components.

References:

1. A.R.E.A. Manual of Recommended Practice, Chapter 15, Part 7, Clause 7.3.4.2 Fatigue, P. 15-7-11, 1984, American Railway Engineering Association, Chicago, Ill.

2. Out, J.M.M., Fisher, J.W., and YEN, B.T. (1984) "Fatigue Strength of Weathered and Deteriorated Riveted Members" Fritz Lab Report No. 483-3, Lehigh University, Bethlehem, Pa.

3. Fisher, J.W., Yen, B.T., Wang, D., Mann, J.E., "Fatigue and Fracture Evaluation for Rating Riveted Bridges", (1987) N.C.H.R.P. Report 302, Transportation Research Board, Washington, D.C.

4. Albrecht, P., and Xu, G., "Fatigue Strength of Long-Term Weathered Rolled Beams" (1986) "Final Report to Maryland Department of Transportation", Dep't of Civil Engineering, University Maryland, College Park, Maryland.

5. Brühwiler, E., Smith, I.F.C., and Hirt, M.A., "Fatigue and Fracture of Riveted Bridge Members", J. of Structural Div. A.S.C.E. P.198-214, January 1990, New York, N.Y.